minerals

MDPI

Article

Early Triassic Episode of the Kresty Volcano–Plutonic Complex Formation in the Maymecha-Kotuy Alkaline Province, Polar Siberia: Geochemistry, Petrology and Uranium–Lead Geochronology

Anatoly M. Sazonov [1], Igor F. Gertner [2], Agababa A. Mustafaev [2,*], Tatyana S. Krasnova [2], Yurii V. Kolmakov [2,3], Cole G. Kingsbury [2] and Vera A. Gogoleva [2]

[1] Department of Geology, Mineralogy and Petrography, Siberian Federal University, 660041 Krasnoyarsk, Russia; sazonov_am@mail.ru
[2] Department of Geology and Geography, Tomsk State University, 634050 Tomsk, Russia; labspmggf@gmail.com (I.F.G.); science@mail.tsu.ru (T.S.K.); kolmakovyv@tpu.ru (Y.V.K.); thecgkings317@gmail.com (C.G.K.); krylova.vera1994@yandex.ru (V.A.G.)
[3] Department of Geology and Geophysics, Tomsk Polytechnic University, 634050 Tomsk, Russia
* Correspondence: alishka010593@gmail.com

Abstract: The Kresty volcano–plutonic complex (KVPC) is one of the representatives of the alkaline–ultrabasic magmatism in the Maymecha-Kotuy Alkaline Province in Polar Siberia. The geological structure of the KVPC consists of intrusive formations of olivinite–pyroxenite and melilitolite–monticellitolite bodies, a series of rocks that break through dikes of trachydolerites, syenites, granosyenites, alkaline picrites and lamprophyres. This paper summarizes the results of the authors' long-term research on the geological structure and features of the material composition of the intrusive magmatic rocks, including geochemistry, mineralogy, distribution of rare earth elements (REE), as well as the results of isotope studies. The multielement composition of the KVPC intrusions demonstrates a complex geodynamic paleoenvironment of the formation as plume nature with signs of subduction and collision. For the ultrabasic series with normal alkalinity from the first phase of the KVPC, a Sm-Nd isochron age yielded an Early Triassic (T_1) result of 251 ± 25 Ma. Here, we present U-Pb dating of zircons and perovskite of high-calcium intrusive formations and a dyke complex of alkaline syenites. Thus, for the intrusion of kugdite (according to perovskite), the age determination was 249 ± 4 Ma, and for the crosscutting KVPC dykes of syenites (according to zircon) 249 ± 1 Ma and 252 ± 1 Ma. The age of the most recent dike is almost identical to the age of the main intrusive phases of the KVPC (T_1), which corresponds to a larger regional event of the Siberian LIP—251 Ma. According to isotopic Sr-Nd parameters, the main source of KVPC magmas is a PREMA-type material. For dyke varieties, we assume there was an interaction of plume melts with the continental crust. The new age results obtained allow us to further constrain the episodes of alkaline–ultrabasic intrusions in Polar Siberia, taking into account the interaction of mantle plume matter and crustal material.

Keywords: Maymecha-Kotuy Alkaline Province; Kresty volcano–plutonic complex; ultrabasic-basic rocks; Siberian LIP; U-Pb age of perovskite and zircon

Citation: Sazonov, A.M.; Gertner, I.F.; Mustafaev, A.A.; Krasnova, T.S.; Kolmakov, Y.V.; Kingsbury, C.G.; Gogoleva, V.A. Early Triassic Episode of the Kresty Volcano–Plutonic Complex Formation in the Maymecha-Kotuy Alkaline Province, Polar Siberia: Geochemistry, Petrology and Uranium–Lead Geochronology. *Minerals* **2024**, *14*, 83. https://doi.org/10.3390/min14010083

Academic Editor: Anastassia Yurievna Borisova

Received: 15 November 2023
Revised: 7 January 2024
Accepted: 8 January 2024
Published: 11 January 2024

1. Introduction

The Maymecha-Kotuy Alkaline Province is a unique natural site where many minerals are concentrated, including chromites, titanomagnetites, apatites, rare earth and precious metal ores. To a certain extent, it acts as an analogue of the Kola Alkaline Province. Its uniqueness is due to the paleogeodynamic environment of rifting in Precambrian cratons associated with one of the largest superplumes in Earth history, the Siberian Superplume. It provoked the Earth's largest mass extinction event, permanently transforming the Earth's biota [1,2]. This superplume initiated rift systems not only in the Khatanga Trough, but also

in Western Siberia [3,4]. Certain remnants of this plume are manifested in the Kuznetsk Trough, the Altai Mountains and in China [1,5,6].

One of the aspects of large igneous province (LIP) formation relates to the duration of active magmatism. Pulses of LIP-related magmatism associated with the involvement of a mantle plume generally do not exceed 5 Ma. According to many sources in the literature [1,7–9], active magmatism at 250 Ma within the Siberian platform was of short duration, lasting no more than 1–2 Ma [1]. These data are based on the results of U-Pb isotope dating of rocks of the Norilsk ore node [10,11], the Guli pluton [7] and individual volcanic strata of the Putorana plateau [12]. This is also confirmed by our research on the unique Kresty volcano–plutonic complex (KVPC).

The earliest studies of the age boundaries of the formation of ultrabasic, alkaline and dyke rocks of the KVPC were based on paleomagnetic studies, the results of which gave a wide age range from 260 to 180 Ma. At the same time, the youngest ages were obtained for dykes of alkaline syenites and granosyenites (these results were not published in the open press, but only given in production reports). Isotopic dating was determined for the Guli pluton and concerned the main intrusive phases and carbonatites completing the formation of this plutonic feature [1]. In this contribution, we have three main objectives: the first objective is to describe the general characteristics of the KVPC, considering previously obtained [1,13] data and new data on petrographic discrimination of the rocks composing this pluton. Our second objective is to compare the incompatible element variations in the KVPC with other massifs (plutons) in polar Siberia in order to arrive at a genetic model of KVPC alkaline magmatism and its ore deposits. Our final objective is to determine the age and magmatic source of the acidic rocks of the dyke complex associated with the KVPC. These formations, as a rule, are considered melting products of crustal material.

2. Geological Setting

2.1. Geological Setting of the Maymecha-Kotuy Alkaline Province

The Maymecha-Kotuy Alkaline Province unites a series of intrusive massifs composed of ultrabasites with normal alkalinity, high-calcium rocks of the kugdite–uncompagrite–melilitolite series, foidolites, alkaline basites, alkaline syenites, granosyenites and carbonatites. The largest intrusion is the Guli pluton, which is exposed on the surface for at least 1200 km^2. Only a part of this pluton is exposed in the structures of the Siberian craton. At least half of it is concealed under the Cenozoic deposits of the Khatanga trough. The remaining bodies are much smaller and their area does not exceed 3–7 km^2. Some of them are localized within the volcanogenic strata, while others break through the carbonate deposits of the Siberian craton cover.

Many researchers have studied the specifics of the geological and tectonic structure of the Maymecha-Kotuy Alkaline Province [4,14–16] with varying explanations regarding the intervening tectonic development. Earlier studies [14] suggested the formation of rift structures in this region to be a rather chaotic distribution of discontinuous faults (such as local rift zones with predominant right-lateral and local left-lateral transform faults). There are several options for interpreting this tectonic activity. For example, some researchers have noted that the faults have a radial orientation and suggested that the focus of this radial pattern delineates the center of the Siberian Superplume at the location of the Guli pluton [2]. However, we focus on the results of the deep gravity exploration, which were obtained by T.M. Chudinova (1993) [15] and interpreted by A.M. Sazonov and coauthors [16]. According to these results, the formation of the Maymecha-Kotuy Alkaline Province is controlled by the transform fault of the main Pyasingo-Khatanga rift system (Figure 1).

The geophysical map in Figure 1 clearly shows a ring gravitational anomaly associated with the transform fault and its proximal location to the Guli pluton. A similar anomaly is observed on the northern flank of the rift structure within the Taimyr Peninsula. The Khaeralakh fault in the west of this structure corresponds to the formation of the Norilsk ore node with rich copper–nickel and noble-metal mineralization. Unique characteristics of

the two observed transform faults of this rift structure are the two gravitational anomalies within the area of trap magmatism in this region. Both transform faults are characterized by a left-lateral sense of displacement along the main rift structure. Between them, there is a fairly large massif of trap basalts, known as the Putorana Plateau. No real ore deposits have yet been identified in this region. The structure of the northern rim of the Siberian craton is represented by volcanic formations. Figure 2 shows the ratio of the thicknesses and broad geochemical affinities of the sections of volcanic in the Norilsk and Maymecha-Kotuy regions with potential correlation of their age and stratigraphic positions.

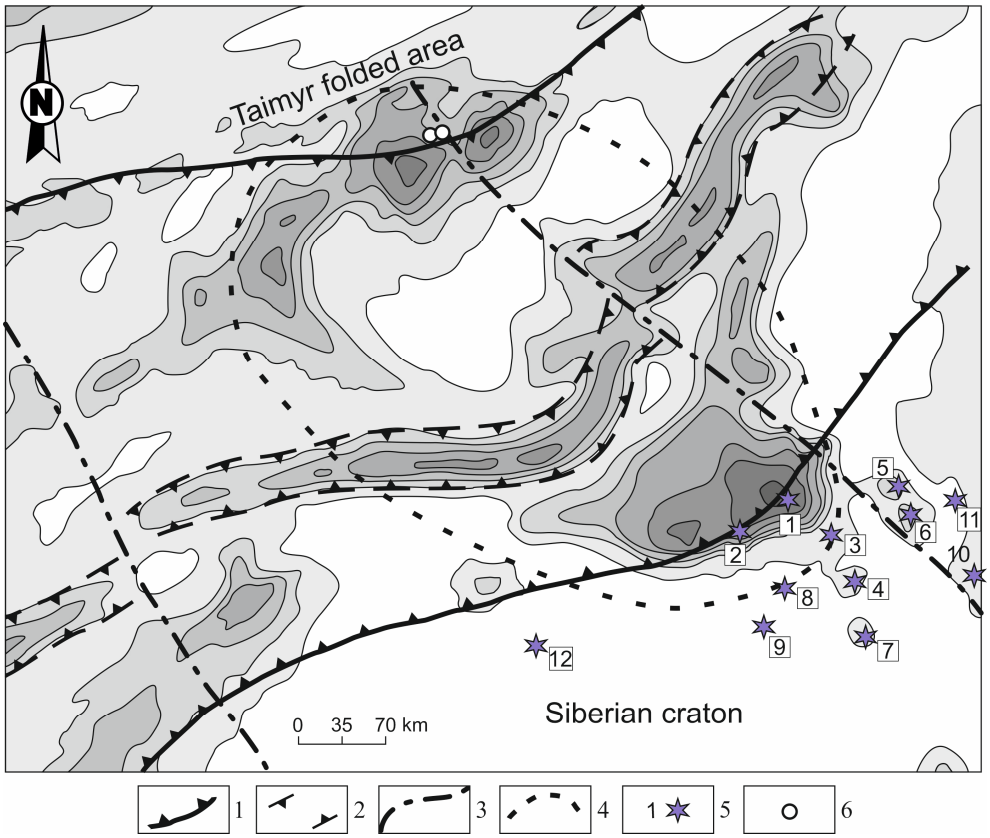

Figure 1. The gravitational field of the Yenisey Khatanga trough according to [15]: 1.—the boundaries of the Yenisey-Khatanga trough; 2.—the boundaries of the middle spreading zone of the Pyasingo-Khatanga rift system; 3.—transform faults; 4.—the contours of the proposed deep ring structure; 5.—alkaline–ultrabasic plutons (1.—Guli pluton; 2.—KVPC; 3.—Sedete; 4.—Dalbykha; 5.—Odinchikha; 6.—Kugda; 7.—Bor-Uryakh; 8.—Romanikha; 9.—Changit; 10.—Magan; 11.—Churbuka; 12.—Kamensk group); 6.—intrusions of subalkaline traps of Taimyr.

The main differences between the Norilsk and Maymecha-Kotuy sections is that the latter has a higher proportion of volcanics that are of alkaline and ultrabasic composition of the volcanic, notably in the upper part of the section of the Maymecha-Kotuy Alkaline Province represented by the Delkansky and Maymechinsky formations. This fact determines the specifics of this region, where the main alkaline–ultrabasite plutons of the province are concentrated.

The fabric of the northwestern fragment of the Siberian craton is largely affected by the development of trap magmatism represented by these volcanic formations. Their ages, according to a number of elements of local isotopic data in alkaline volcanic, fits into a rather tight time interval of 251–252 Ma. This, in many ways, defines the duration of the activity of the Siberian Superplume [17].

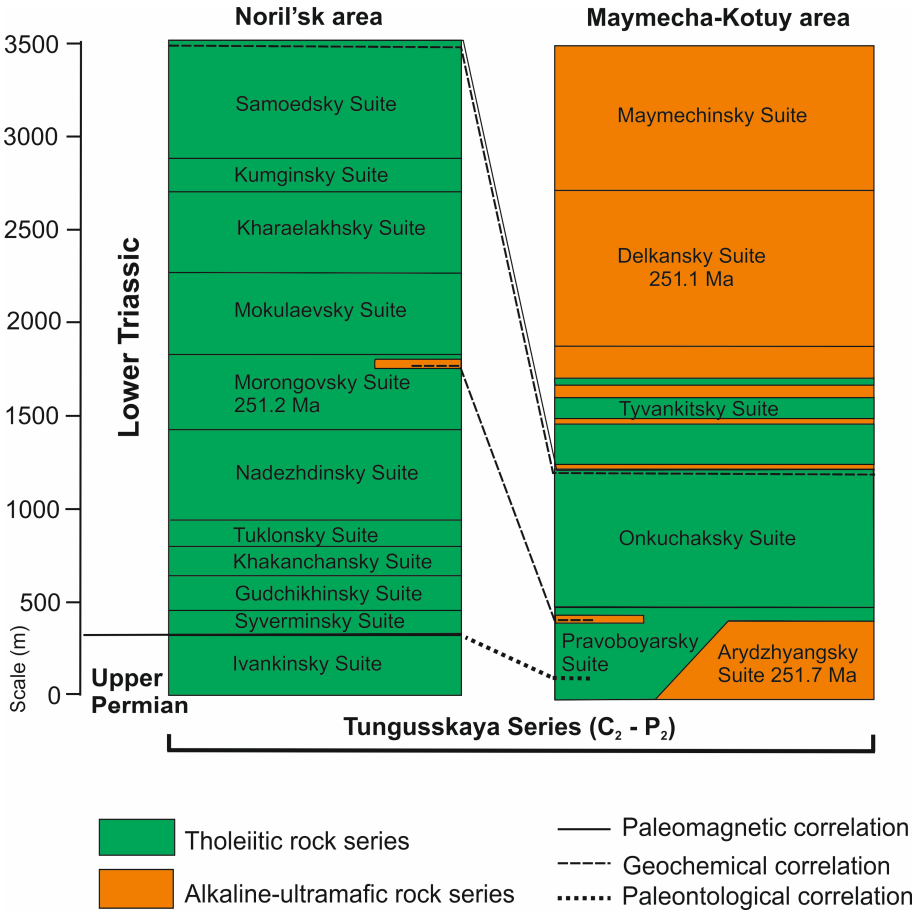

Figure 2. Correlation of sections of the volcanic complexes in the Norilsk and Maymecha-Kotuy areas in the Northern outskirts of the Siberian Platform by [1].

2.2. The Internal Structure of the Kresty Volcano–Plutonic Complex

The structural features of the alkaline–ultrabasic KVPC and the fabric of its constituent rocks are studied in detail in the monograph "Platinum-bearing alkaline-ultrabasic intrusions of Polar Siberia" [16], which were published in Russian in a small edition (~300 copies). These results are rather poorly presented in the foreign literature. Therefore, in this article, we present the most significant results of our early studies and new U-Pb age determinations of rocks from the KVPC, which confirm the short duration of magmatism in the Maymecha-Kotuy Alkaline Province. In addition, intrusive, metamorphic and metasomatic formations of the junction zone between the northwestern part of the Anabaro-Olenek anticline, the northeastern part of the Tungus syncline, and the southwestern side of the Yenisey-Khatanga regional trough (which includes the Maymecha-Kotuy Alkaline Province) were described in detail by the staff of the A.P. Karpinsky Russian Geological Institute (VSEGEI) cartographic factory, during the creation of the State Geological Map of the Russian Federation, scale 1:1,000,000 (third generation), Norilsk series, sheet R-47–Heta [18].

From a regional perspective, the KVPC can be considered a "satellite" of the Guli pluton, because it is located in close proximity to it (~54 km) and has a similar petrographic composition, including two main intrusive phases presented by olivinite–wehrlite–pyroxenite and kugdite–melilitolite complexes. The only difference is the presence of a monticellitolite body on its northern flank. Just like the Guli pluton, the KVPC is only partially exposed in the structure of the Siberian craton, the rest of it concealed under younger Cenozoic deposits of the Khatanga trough. Its ring structure is reflected in the geomagnetic field, which was interpreted by Y.V. Kolmakov [16]. KVPC cross-cuts the alkaline volcanic of the Delkan formation and is represented by melanonephelinites with local fragments of

nephelinites, trachybasalts and trachytes. Intrusive contact with the host stratum is confirmed by a fine-grained hornfels zone of melteigite-ijolite. The main intrusive phases of the massif are: (a) banded olivinite–wehrlite–clinopyroxenite complex; (b) a later intrusive phase, represented by high–Ca rocks with increased alkalinity of the "kugdite–melilitolite–monticellitolite" series. A more detailed structure of the KVPC is shown in Figure 3.

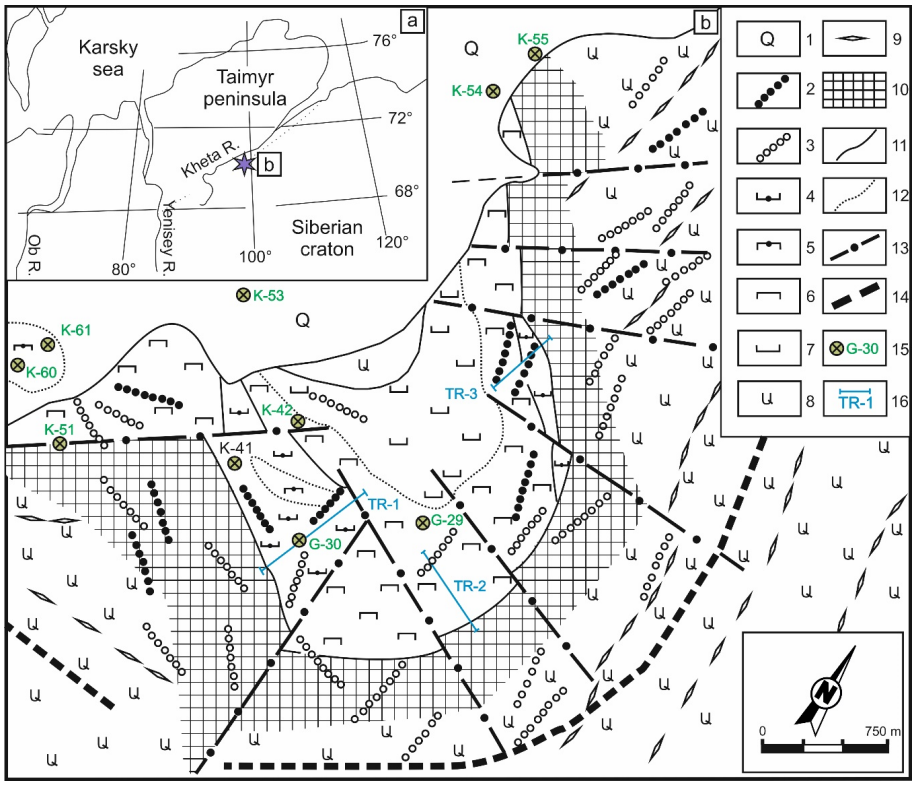

Figure 3. The location of the KVPC on the territory of polar Siberia (**a**) with a detailed geological scheme according to [16] with the following amendments by the authors (**b**): 1.—loose deposits KZ; 2–9.—volcanoplutonic rocks MZ_1: 2.—dykes of alkaline syenites and granosyenites; 3.—dykes of trachydolerites and trachyandesites; 4.—kugdite and melilitolite; 5.—monticellitolite; 6.—banded olivinite–wehrlite–clinopyroxenite complex; 7.—olivinite; 8.—melanonephelinite; 9.—local fluxes of melanonephelinite volcaniclastics; 10.—hornfels; 11.—geological boundaries; 12.—bound areas between petrographic variations within intrusive bodies; 13.—faults; 14.—KVPC boundaries by gravity data; 15.—boreholes and their numbers; 16.—trenches and their numbers.

The intrusive contact between the first and second phases is confirmed by the development of hybrid varieties such as melilite-containing olivinites or uncompagrites. The monticellitolite body has a unique location; it is exposed in the northern flank of the KVPC by two drill cores. The relationship with the main body of kugdites has not yet been established, but the homogeneity of these rocks suggests their autonomous formation. The structure of the KVPC is complicated by a series of tectonic deformations and trachydolerite, syenite and granosyenite dykes oriented in the north-west and north-east directions. These orientations correspond to the orientation of the rift structure of the Khatanga trough and the transform fault that cross-cuts it (Figure 1).

The fabric of the pluton and the enclosing volcanic melanonephelinite and nephelinite strata with separate layers of trachybasalts and trachyandesites allow us to consider this object as an independent KVPC structure. Previously, age data were obtained by paleomagnetic studies (stock unpublished results), the results of which reflected a protracted period of magmatism associated with the KVPC (from 250 to 170 Ma). Moreover, the dykes of syenites and granosyenites showed the youngest ages. More reliable geochronological parameters were obtained on the basis of Sm-Nd isochron data for rocks of the banded

ultrabasic series yielding a result of 251 ± 20 Ma [13]. The new results of U-Pb dating confirm the short-term duration of alkaline magmatism in the Maymecha-Kotuy Alkaline Province, using the example of the KVPC and taking into account the late high-silica dykes.

3. Materials and Methods

The concentrations of petrogenic elements were measured by XRF at the Institute of Geology and Mineralogy of the V.S. Sobolev Siberian Branch of the Russian Academy of Sciences (Novosibirsk, Russia) on an ARL-9900XP X-Ray Fluorescence (XRF) apparatus. X-ray fluorescence silicate analysis was performed from fused pellets: the analyzed sample was dried at 105 °C for 1.5 h, then annealed at 960 °C for 2.5 h and then mixed with flux (66.67% lithium tetra borate; 32.83% lithium meta borate and 0.5% lithium bromide) in a ratio of 1:9 (the total weight of the mixture was 5 g). The mixture was melted in platinum crucibles in a Lifumat-2.0-Ox induction furnace according to the standard method [19].

Rare and trace elements were measured by ICP-MS at Tomsk Regional Core Shared Research Facilities Center of the National Research Tomsk State University (Tomsk, Russia) on an Agilent 7500 inductively coupled plasma mass spectrometer (ICP-MS). The center was supported by the grant of the Ministry of Science and Higher Education of the Russian Federation 075-15-2021-693 (No. 13.RFC.21.0012). To perform mass spectral analysis with inductively coupled plasma, a 0.1 g sample was treated with 10 mL of HF acid with a 4-h exposure in an open system at a temperature of 70 °C, after which 2 mL of HNO_3 concentrate was added. The samples were exposed to microwave action in a closed system at a power of 700 W with a gradual increase in temperature to 200 °C. After this, the sample was evaporated to dryness, treated twice with 6.2 M HCl, then evaporated again and treated with concentrated HNO_3. The dry residue was then transferred to a solution of 15% HNO_3. Indium was used as an internal standard. Immediately prior to ICP-MS analysis, the sample was diluted by nitric acid to yield a concentration of 3%. The dilution factor was 1000 [20]. Error rates in the sample for the measurement range from 0.001 to 0.1 ppm are not more than 0.39%, over 0.1 to 10 ppm are not more than 0.32%, over 10 to 500 ppm are not more than 0.21% and over 500 to 50,000 ppm are not more than 0.17%. The accuracy rate corresponds to 0.95%.

The U-Pb isotopic analysis of zircon from syenites and perovskite from kugdites extracted for age dating was performed on the SHRIMP-II ion microprobe at the VSEGEI Isotope Research Center of the A.P. Karpinsky Russian Geological Research Institute (St. Petersburg, Russia) using a standard technique. Cathodoluminescent images were obtained using an ABT55 scanning electron microscope in a normal operating mode. International geochronological standards (for Temora zircon and for perovskite from the skarn of the Tagheran massif) were used to calibrate U-Pb dating. Optically, backscattered electron (BSE) and cathodoluminescent images reflecting the internal structure and zoning of the grains were used to select the location of local U-Pb dating. The measurement of U-Pb ratios was carried out according to the methodology described in [21]. Data processing was completed according to the SQUID program [22] with normalization of the U-Pb ratio to the standard TEMORA zircon [23] and perovskite [24]. Errors for single analyses (isotope ratios and ages) were estimated in the range ± 1σ, and for calculated concordant ages and intersections with concordia ± 2σ. Processing of the received data was carried out using the SQUID program [22]. The graphs with concordia age were plotted using the ISOPLOT/EX program [22].

4. Results and Discussion

4.1. Petrography of Studied Rocks

Petrographic diversity of the KVPC is represented by rocks of both subalkaline ($Na_2O + K_2O$ = 0.31–1.06 wt.%) and alkaline ($Na_2O + K_2O$ = 4.16–10.45 wt.%) series (Supplementary Materials, Table S1). Melanonephelinites with rare interlayers of standard nephelinites, trachybasalts and trachyandesites act as the main varieties of the volcanogenic component. The intrusive phases are represented by a banded (differentiated) olivinite–we-

hrlite–clinopyroxenite complex, which comprises the marginal fragments of the central portion of the intrusive body. There are ultrabasic bodies represented by a series of "kugdite–melilitolite" and individual fragments of monticellitolites in the core. On the northern flank, these rocks form an autonomous body, which makes it possible to consider them as an independent intrusive phase. Other types of rocks are the host volcanic of the melanonephelinite series, dyke and vein varieties. Dykes are represented by trachydolerites, alkaline syenites and granosyenites, which mark the final magmatic stage of the KVPC. Individual dykes correspond to the composition of melilite and nepheline-containing lamprophyres or carbonatite-like rocks. The origin of the latter is still poorly understood; most likely, they are vein bodies of carbonated monticellitolites because they lack one of the main mineral components in the form of phosphates (apatite and silicates such as pyroxenes or olivine).

Microphotographs in plain-polar (PPL) and crossed polarizations (XPL) of KVPC rocks are shown in Figure 4a–c. The rocks of the olivinite–wehrlite–clinopyroxenite series (Figure 4a–c) are characterized by two main minerals—olivine and clinopyroxene—and a certain presence of accessory minerals—titanomagnetite and perovskite. In a number of individual varieties, the concentration of the latter is 10–40%, which allows them to be attributed to ore varieties of these rocks such as ore olivinite or kosvite. The grain size varies from 0.5 to 2 mm, although there are almost always larger grains up to 3.5–5 mm in size. To some extent, we can also talk about the porphyritic appearance of these rocks. The texture of rocks is usually massif-like (Figure 4a–c). A fabric of this rock corresponds to the panidiomorphic type with elements of sideronite. The amount of olivine grains ranges from 70% to 90%. In the case of ore varieties, the euhedral olivine grains are cemented with an ore component, the amount of the latter can reach about 30–40%. Wehrlites, olivine-containing clinopyroxenites and, in fact, clinopyroxenites are characterized by a hypidiomorphic microstructure, where olivine acts as a constantly more idiomorphic phase (Figure 4b,c). Additionally, elements of sideronite relationships of the main rock-forming and ore minerals are observed, especially for clinopyroxenites.

The rocks of the calcium chemical series *"kugdite–uncompagrite-melilitolite-monticellitolite"* are presented as separate intrusive phases occupying autonomous positions (CaO = 20.26–27.76 wt.%). Interaction with the ultrabasic of normal alkalinity (Na_2O + K_2O = 0.31–1.06 wt.%) (Supplementary Materials, Table S1) is most often determined by melilite-containing olivinites, where the role of melilite is quite limited (no more than 5–7%) or uncompagrites, which contain clinopyroxene. The main minerals in this alkaline–ultrabasic intrusive association "kugdite–uncompagrite-melilitolite-monticellitolite" are olivine, melilite, clinopyroxene and accompanying ore minerals (titanomagnetite and perovskite). The structure of these rocks is determined by the obvious idiomorphism of olivine in relation to melilite and pyroxene with elements of sideronite relationships with ore minerals. The fabric features of these rocks are shown in Figures 4d,e and 5a. In XPL, melilite is characterized with abnormal coloration in bluish or dark brown tones, which reflects its low birefringence and dispersion. For monticellitolites, microstructural features are preserved where olivine grains are the most idiomorphic.

The *monticellitolites* form an autonomous body, which was exposed by two drill cores to 100 m deep [16]. At the same time, these rocks have a massif texture and a homogeneous structure, which allows us to talk about an independent intrusive phase. Contacts with a probable relationship with a body of kugdite–melilitolite composition have not been studied. A distinct petrofabric is defined by the presence of rare euhedral olivine crystals and the predominant panidiomorphic grains of monticellite. Magnetite acts as an accessory mineral (Figure 5a).

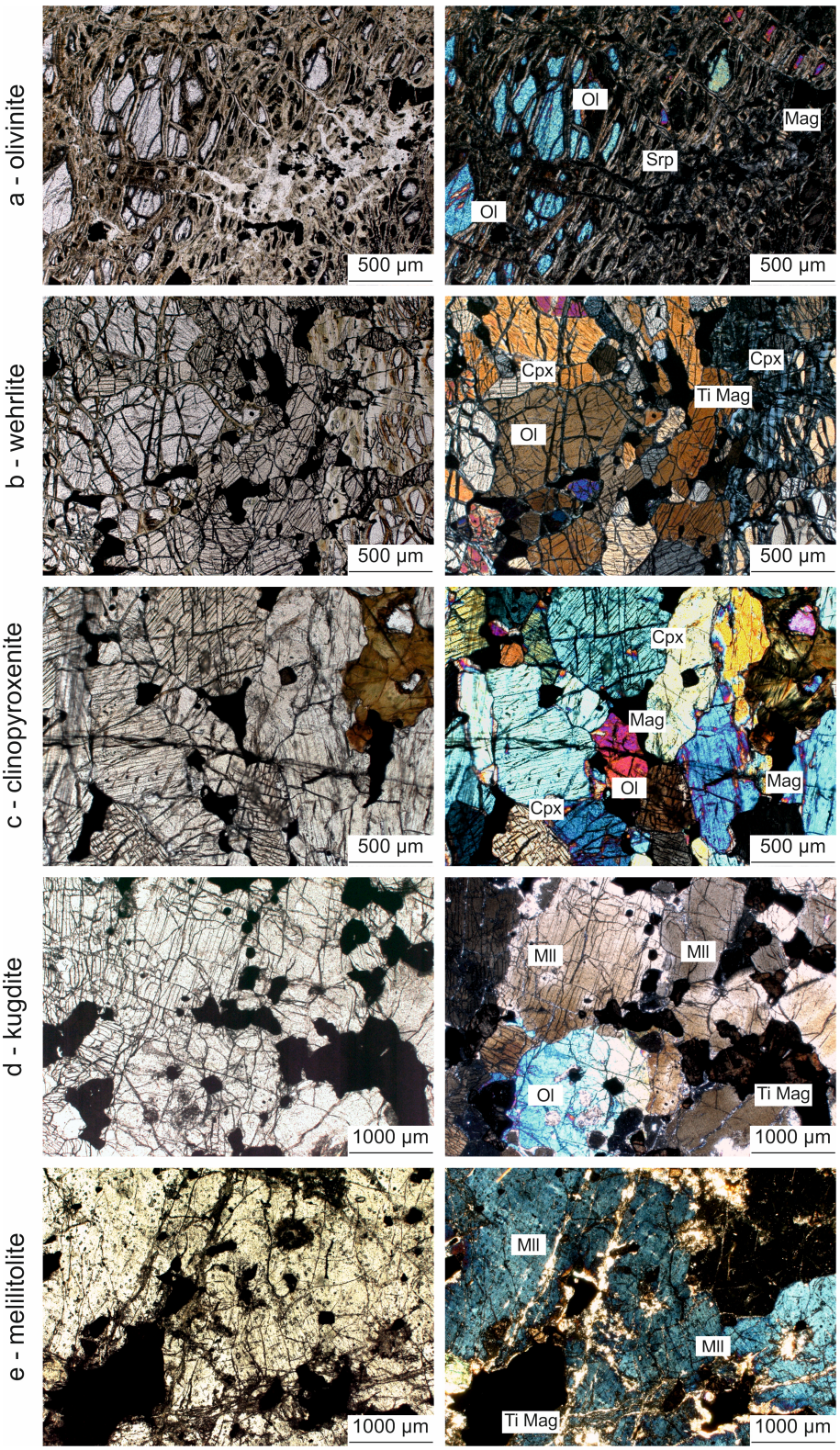

Figure 4. Photomicrographs of thin sections from the main intrusive phases from the KVPC: (**a**–**c**)—ultrabasic rocks of normal alkalinity, representing the series "olivinite–wehrlite–clinopyroxenite"; (**d**,**e**)—rocks of the high-calcium series "kugdite–melilitolite". The photomicrographs were taken in PPL (left side) and XPL (right side) polarization. Key to mineral abbreviations as given according to [25]: Ol—olivine; Mg—magnetite; Spr—serpentine; Cpx—clinopyroxene; Ti Mag—titanomagnetite; Mll—melilite; Mag—magnetite.

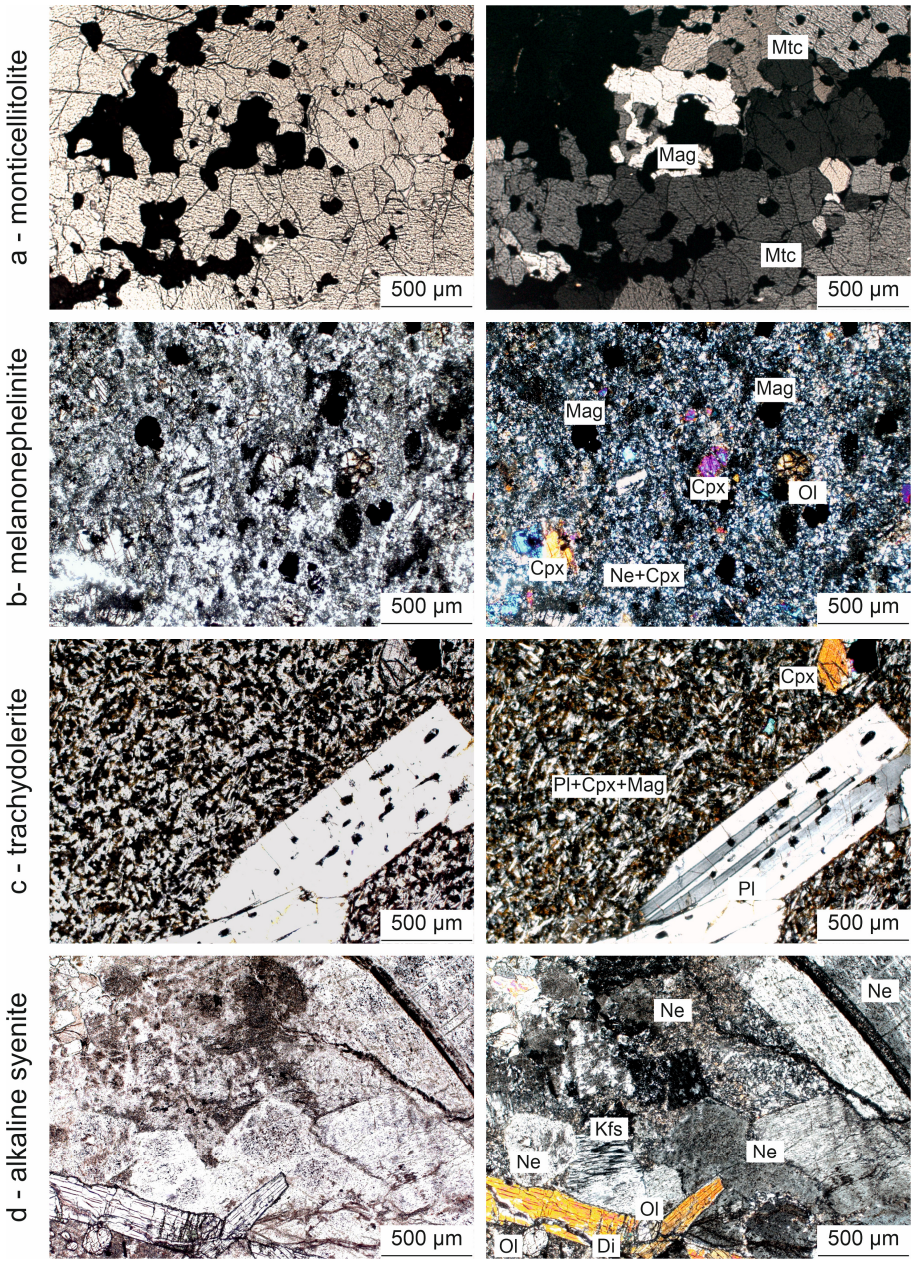

Figure 5. Photomicrographs of monticellitolites containing effusive and dyke varieties of the KVPC: (**a**)—monticellitolite; (**b**)—melanonephelinite; (**c**)—trachydolerite; (**d**)—alkaline syenite. The photos were taken in PPL (left side) and XPL (right side) polarization. Key to mineral abbreviations are given according to [25]: Mtc—monticellite; Mag—magnetite; Pl—plagioclase; Kfs—K-feldspar; Ne—nepheline; Ol—serpentized olivine; Di—diopside.

The rocks of the enclosing volcanogenic strata are represented by alkaline rocks of the "melanonephelinite and nephelinite" series (Figure 5b). A characteristic feature of these volcanic rocks is the porphyritic texture is due to the presence of large clinopyroxene phenocrysts relative to the groundmass, and nephelinites are characterized by the presence of nepheline phenocrysts. Directly in contact with an ultrabasic body, they recrystallize in the form of fenitized fine-grained ijolite or melteigite. Diopside in nephelinites often acquires a greenish color and slightly elevated contents of aegirine (up to 2–3%).

The rocks of the dyke and vein series are quite diverse in petrographic composition (Figure 5c,d). In this case, we describe only the most common—*trachydolerites and alkaline syenites* (selvsbergites). The latter varieties act as one of the final phases of magmatic activity during the formation of the KVPC, for which U-Pb age determination studies were completed (see Section 4.4). Among the dykes of *trachydolerites*, several varieties are observed, differing in the degree of crystallization. Separately, trachybasalts, aphyric trachydolerites, poikilitic trachydolerites and subalkaline plagioclase porphyrites can be distinguished. Their mineral and chemical compositions are quite similar, so we are only providing a description for the most granular varieties. As a rule, clinopyroxene of the diopside type and plagioclase crystals are present as phenocrysts (Figure 5c,d). The bulk is characterized by a poikilitic texture with an explicit idiomorphic of the main plagioclase. Trachydolerites form separate dyke bodies. The features of their petrographic composition are defined by the presence of olivine and clinopyroxene inclusions, but to a greater extent by significantly large crystals of plagioclase. The bulk is characterized by interstitial microstructure, which is dominated by microlites of plagioclase, clinopyroxene and ore mineral (Figure 5c). *Alkaline syenites* are represented by fine-grained rocks with elements of porphyritic texture. According to their mineralogical composition, they are selvsbergites. Orthoclase with signs of perthite texture, plagioclase (from albite to andesine), dark-colored minerals (diopside to augite with a small component of an alkaline mineral such as akmite or aegirine, as well as biotite) and accessory ore minerals are found in the rocks. As secondary changes, the development of hornblende of the uralite–actinolite type (Figure 5d) is often noted. Accessory minerals are titanomagnetite, apatite and zircon.

4.2. Chemistry Composition of Rock-Forming and Ore Minerals

The main minerals of the ultrabasic and high-calcium petrochemical series are olivine, clinopyroxene, melilite, monticellite and accessory minerals. First of all, we consider rock-forming minerals and their probable variations. The composition of olivine in the series of "olivinite–wehrlite–clinopyroxenite" corresponds with a fayalite composition of 9 to 16%. A similar trend can be traced for calcium ultrabasic rocks and host nephelinites. A typical feature is the increased concentrations of CaO (CaO = 0.3–1.0 wt.%). This aspect reflects the subvolcanic nature of the magmatic complex. In the kugdite–melilitolite association, there is a weakly expressed accumulation of calcium oxide with an increase in melilite (CaO = 1.7 wt.%). However, it does not imply any pattern. The Ni content, as well as Mn, depends on the ferruginous content (mafic index) of olivine. It was previously noted that in the most magnesian varieties of this mineral the concentration of NiO ranges from 0.01 to 0.16 wt.%, and in the most ferruginous, the content of MnO reaches 0.4 wt.% [16].

The composition of clinopyroxene is close to the stoichiometric formula of fassaite reflecting the predominance of wollastonite over enstatite. Its mafic index, in general, corresponds to the parameters of olivine. Additionally, we note the constant presence of alkaline oxides at the level of 0.2–0.4% with a sharp predominance of the sodium component.

The composition of melilite corresponds to the "galena-akermanite" series with the chemical formula $Ca_{1.18–1.83}Mg0_{0.6–0.75}Al_{0.14–0.19}Fe0_{0.07–0.12}Na_{0.16–0.21}Si_{2.0–2.05}$ [16]. One of the distinctive features of KVPC melilite in contrast to other alkaline- ultrabasic plutons of the province (Kugda, Nemakite, Odihincha and others) (Figure 1) is the reduced concentrations of Al. One of the variants of such genesis may be the interaction with the carbonate substrates of the Siberian craton, which these objects are localized in [26]. Quite often such examples are observed for folded areas of alkaline magmatism [6,27,28].

The composition of monticellite varies. It is present in the form of reaction rims in the structure of melilitolites, in silicate inclusions in olivine in the form of separate vein bodies among kugdites, as well as independent grains within the olivine–monticellitolite rocks. As a rule, the composition of this mineral corresponds to its formula and assumes close ratios of calcium and magnesium oxides. Most often, there are differences in its ferruginous component. The content of fayalite in microlites of silicate inclusions varies from 5.1 to 17.7 wt.%. For other formations, they fit into a narrower range (from 10 to 18 wt.%). The average

mineral formula can be presented as follows: $Ca_{0.91–0.99}Mg_{0.76–0.99}Fe_{0.05–0.09}Si_{0.98–1.02}$ [16]. Impurities of other components make up the first hundredths of one percent, or simply are not determined at the level of the microprobe analysis error.

As a rule, ore minerals are presented by titanomagnetite and perovskite, whose content reaches the level of rock-forming elements (up to 10–30 wt.%). These types of rocks are distinguished as independent in the form of ore olivinites, kosvites, ore melilitolites or monticellitolites. In addition to these oxides, chromite, ulvospinel and magnetite are present in small quantities. Titanomagnetite is present in two forms. The first form is as small grains within idiomorphic inclusions, while the second form is as a mineral which exists within interstices between the main rock-forming minerals. Additionally, this mineral is intermediate in the series "magnetite–titanomagnetite–ulvospinel". The TiO_2 content ranges from 2.3 to 16.4 wt.% in magnetite and its titanium variety. In ulvospinel and ilmenite, it reaches 33–46 wt.%. The most common impurity is Al_2O_3 (0.3–3.4 wt.%), MnO (0.3–2.7 wt.%), Cr_2O_3 (0.0–6.8 wt.%) and CaO (0–1.6 wt.%). The most interesting aspect is the presence of Au (up to 1.8 ppb) [13,16,26]. In many ways, perovskite is like titanomagnetite. It also forms as inclusions within olivine, clinopyroxene and melilite, and exists within interstices in ore varieties of rocks.

A typical feature for the rocks of the KVPC is also the presence of precious minerals (gold and platinum group metals). Most often, they are confined to secondarily altered rocks, where disseminated mineralization is recorded with the development of pyrrhotite, pentlandite, pyrite, chalcopyrite, galena, sphalerite, as well as secondary derivatives such as covellinite, bornite, jerfisherite, chalcosine and hizlewudite. The concentration of these minerals is rather insignificant, which allows us to speak about their accessory nature and the superimposed post-magmatic metasomatic processes. Out of the noble metal mineralization, the most common are native Au with impurities of Sb and Hg of different purities from 819 to 990 ‰, platinum and iron alloys, Ru-Ir alloys and Os. Finally, we note the presence of native Fe and graphite which suggests these play a role in the formation of alkaline–ultrabasic rocks and CO_2 with subsequent reduction to pure carbon [26].

4.3. Geochemistry

The chemical parameters according to the classic two- and three-component diagrams fully correspond to the parameters determined by the mineralogical and petrographic composition of rocks from the KVPC (Figure 6). The deviation can be considered to be wehrlites falling into the field of basic rocks, but it depends on the plotting specifics of certain diagrams [29]. In most cases, melanonephelinites and nephelinites, as well as kugdites, melilitolites and monticellitolites are characterized as products of the alkaline and subalkaline magmatic series. Ultrabasic and basic rocks have typically reduced concentrations of alkaline elements.

Nevertheless, lanthanide concentrations are higher for them, especially for calcium-rich rocks (clinopyroxenites, kugdites, monticellitolites) (CaO = 20.26–27.76 wt.%; ∑REE = 2004.57–6018.76 ppm) (Supplementary Materials, Table S1). Very often, the figurative points of compositions of various varieties are at the boundary between normal alkalinity, sub-alkaline and alkaline series products. Again, this is explained by the specifics of the selected parameters in the diagrams [30]. For example, high concentrations of Ti relative to Zr indicate rather low values of this parameter due to the development of titanomagnetite and perovskite, mainly in ultrabasic rocks without significant accumulation of zirconium mineral phases. In this case, baddeleyite and zircon are clearly subordinate in their quantity to the ore components of titanium. On the other hand, a fairly wide distribution of baddeleyite is reflected in comparatively elevated Nb/Y ratio. The observed dispersion of rocks across various fields (Figure 6b) is most likely due to the specifics of the development of ore and accessory minerals. The ternary diagram Ne'–Ol'–Q' [31] shows the results of the normative recalculation of the chemical composition of the studied rocks using the PetroGram method [32]. The compositions of kugdite and monticellitolite either shift towards or are close to the field of subalkaline rocks, and trachydolerites move into the

alkaline field (Figure 6c). In this case, it is explained by the specifics of the calculation with the determination of the larnite mineral in high-calcium ultrabasic rocks and a significant presence of alkaline feldspar. Modern methods of XRF do not separate the ferrous and ferric iron, which leads to a deficiency in silicon and the visible appearance of nepheline (when recalculating the iron components). In reality, the ratios of minerals are observed, which are recorded during petrographic studies.

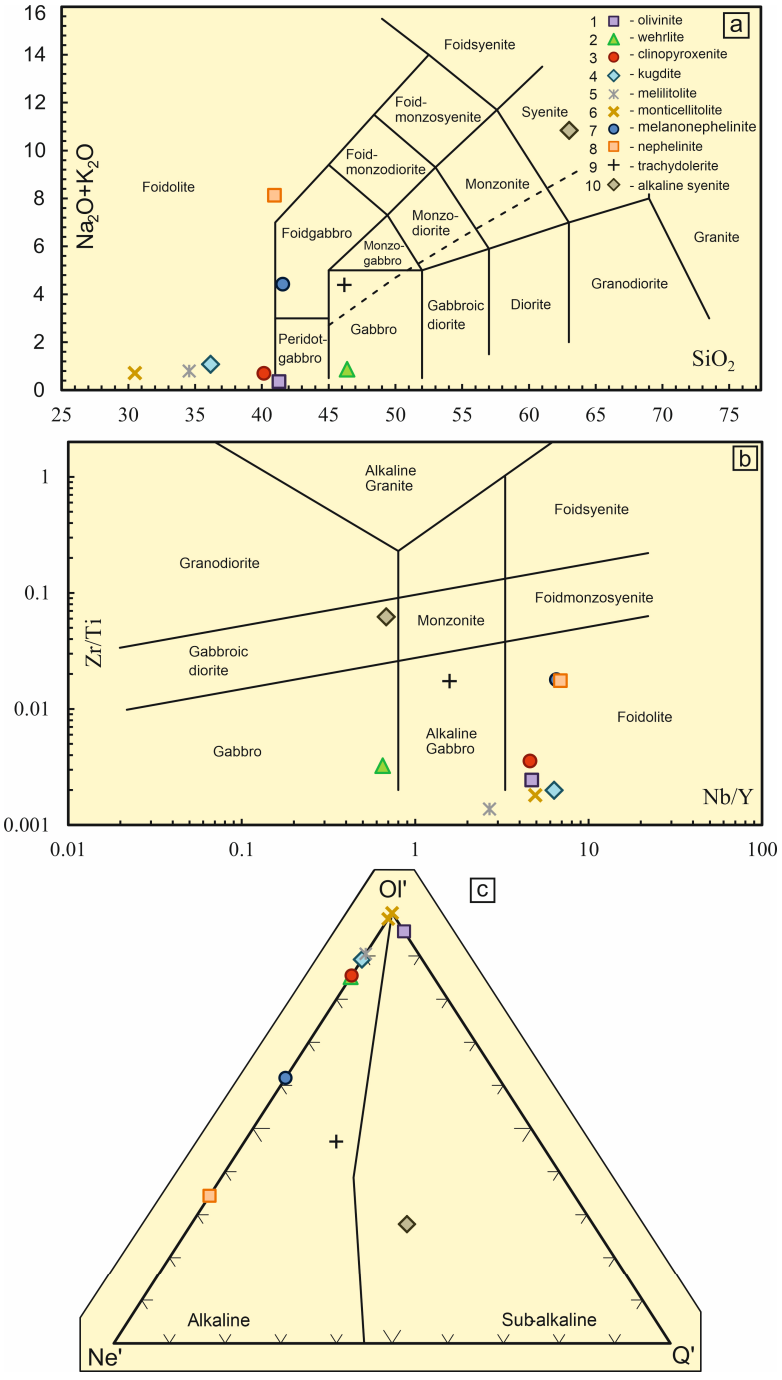

Figure 6. Chemical compositions of the studied rocks of the KVPC: (**a**)—total alkali-silica (TAS) classification diagram (SiO_2 vs. $Na_2O + K_2O$) [29]; (**b**)—Nb/Y vs. Zr/Ti classification diagram [30]; (**c**)—the Ne′–Ol′–Q′ ternary diagram. [31].

According to the $Mg^{\#}$ vs. Ti diagram, two composite fields can be seen (Figure 7a). One of them unites the compositions of monticellitolite, nephelinite, clinopyroxenite, melanonephelinite and trachydolerite, which are characterized by increased Ti = 18,183–25,142.78 ppm with relatively low $Mg^{\#}$ = 47.49–72.26 wt.%. Kugdite, olivinite, wehrlite and melilitolite have lower concentrations of Ti = 3362.88–8530.31 ppm, along with higher $Mg^{\#}$ = 73.56–80.36 wt.% (Figure 7a). A similar gap in the composition fields is also recorded in other diagrams. The only difference is a series of rocks that differ in parameters. Monticellitolites and olivinites, having increased $Mg^{\#}$ = 72.26–80.36 wt.%, sharply differ in the increased value of CaO/Al_2O_3 = 56.79–58 wt.% from other varieties, which is primarily due to low concentrations of alumina in their composition (Figure 7b) (Supplementary Materials, Table S1).

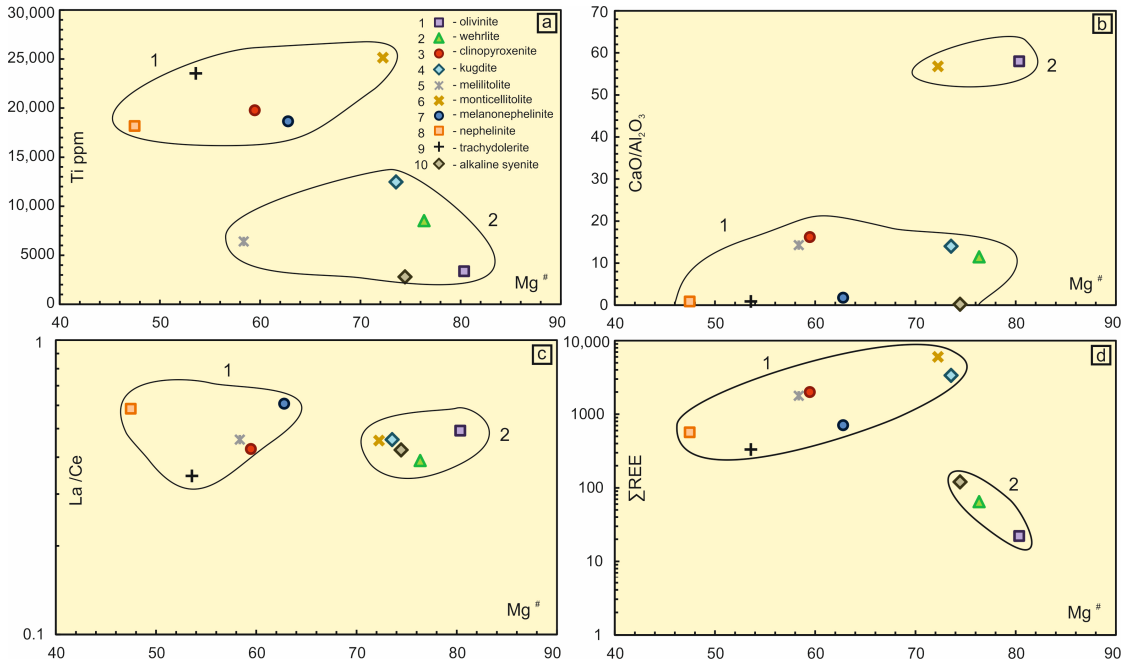

Figure 7. The position of the figurative points of the rocks of the KVPC on binary diagrams: (**a**)—Ti ppm vs. $Mg^{\#}$ wt.%; (**b**)—CaO/Al_2O_3 wt.% vs. $Mg^{\#}$ wt.%; (**c**)—La/Ce ppm vs. $Mg^{\#}$ wt.%; (**d**)—∑REE ppm vs. $Mg^{\#}$ wt.%. The magnesium number $Mg^{\#}$ was calculated by the formula $Mg^{\#}$ = MgO/(MgO + FeOtot) wt.%.

With respect to La/Ce ppm, all rocks of the KVPC have approximately the same values (La/Ce ≈ 0.464 ppm), but they clearly differ in $Mg^{\#}$. At the same time, nephelinites, melanonephelinites, clinopyroxenites, melilitolites and trachydolerites have reduced $Mg^{\#}$ content compared to the field of monticellitolites, kugdites, olivinites and syenites. The nature of the latter is quite interesting and may be related to the impact of the plume during melting of the most acidic varieties at the final stage of KVPC-related magmatism. According to the total accumulation of rare earth elements (∑REE) at a sufficiently high $Mg^{\#}$, syenites, wehrlites and olivinites (∑REE = 22.19–119.97 ppm), which contain minimal amounts of calcium minerals, clearly differ from other varieties. In a field with a high content of ∑REE, two trends can be distinguished. One of them with a lower lanthanide content is "trachydolerite–melanonephelinite–kugdite" (∑REE = 331.34–3376.86 ppm), and the second combines a series of "nephelinite–melilitolite–clinopyroxenite–monticellitolite" (∑REE = 566.51–6018.76 ppm) (Figure 7d).

Multielement geochemical characteristics of common KVPC rocks are shown in Figure 8. The figure shows the distribution of rare earth elements (REE) normalized to chondrite [33]. We note here that ultrabasic rocks of normal alkalinity in addition to trachydolerites and syenites have minimal concentrations of lanthanides exceeding the standard [33]. The REE concentration of the KVPC, as indicated in Figure 8a, demonstrates that

light rare earth elements (LREE) are enriched relative to heavy rare earth elements (HREE) La/Yb = 30.68–67.44 ppm (Supplementary Materials, Table S1). The maximum enrichment was established for high-calcium ultrabasites of the "kugdite–melilitolite–monticellitolite" series, clinopyroxenites and host rocks of KVPC melanonephelinites, respectively, La/Yb = 160.67–698.25 ppm. Their concentration at the LREE level reaches 2000–8000 ppm exceeding the standard of chondrite (Figure 8a). The intermediate position is occupied by nephelinites, trachydolerites and syenites La/Yb = 8.3–96.14 ppm. At the same time, these rocks are characterized with a higher degree of differentiation, which is reflected in the REE spectra, which range from 96 to 100 ppm in nephelinites, up to 350 ppm in clinopyroxenites and reaches 500–700 ppm values in calcium ultrabasites (Figure 8a).

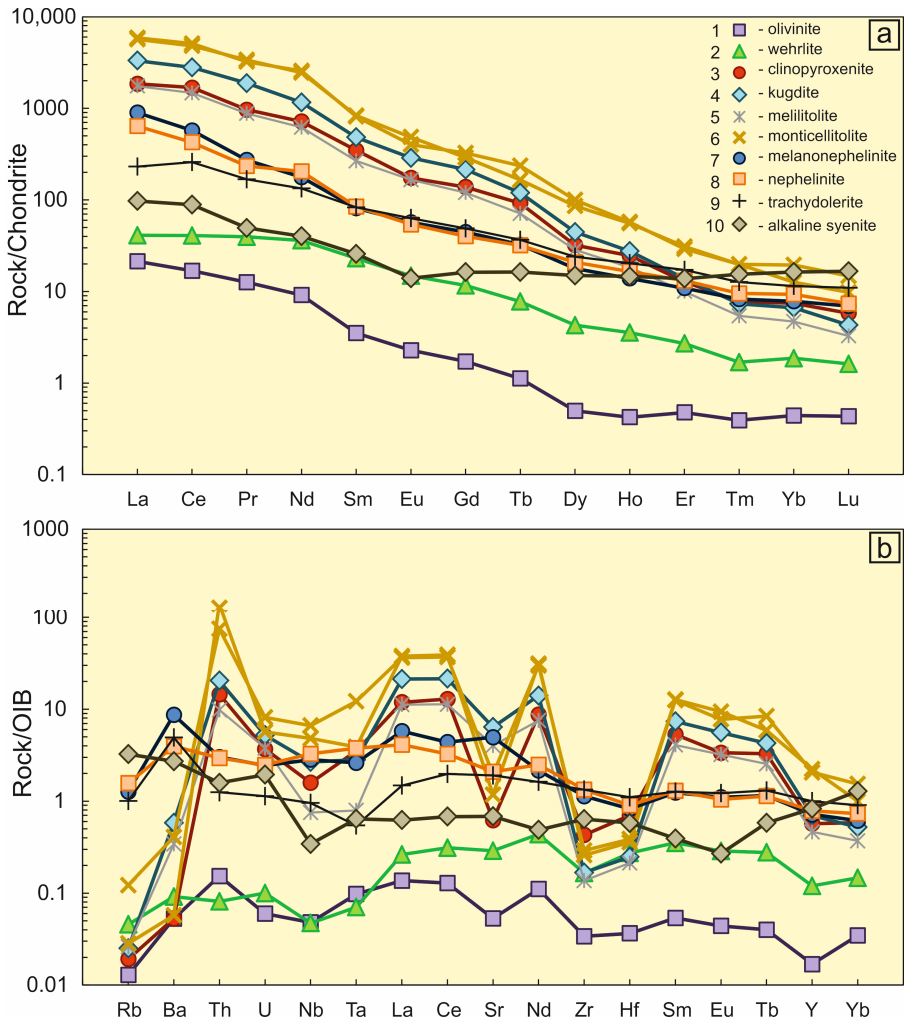

Figure 8. Distribution of rare and rare-earth elements in the magmatic rocks of the KVPC. The normalization was performed for chondrite (**a**) and Ocean island basalts (OIB) (**b**) using the normalization factors of [33].

It is of note that the KVPC rocks lack a negative Eu anomaly in most of the studied rocks. This fact indicates sequential fractionation in the series "olivine–clinopyroxene" and "olivine–melilite–monticellite" without the involvement of plagioclase. The only deviation is the syenite sample, where a weak negative anomaly of this element is recorded. Syenites should probably be considered as a differential of trachyandesite magma, whose dykes are also present in the structure of the KVPC.

A similar pattern is observed for the high-field strength elements (HFSE) plots (Figure 8b). The lowest concentrations relative to the standard of Oceanic island basalts (OIB) [33] are olivinites and wehrlites of the KVPC (∑HFSE = 87.74–335.16 ppm). For trachydolerites, alkaline syenites and host volcanic, the concentration of rare elements (∑HFSE = 1839.78–7511.82 ppm) is comparable to OIB–type basalts. Clinopyroxenites and high-calcium ultrabasites (CaO = 20.26–27.26 wt.%) have a sufficiently differentiated spectrum (∑HFSE = 2590.61–7849.16 ppm), which is characterized by a series of positive and negative anomalies. A clear indicator is increased concentrations of Th and negative anomalies of Sr, Nb, Ta, Zr and Hf, which usually indicate a previously depleted mantle source in a subduction zone setting. This scenario can be considered as a product of the mineralogical compositions, as well as a criterion for determining the paleogeodynamic evolution of the KVPC or the nature of involvement of continental crust with KVPC magmas.

The concentration of precious metals acts as separate geochemical aspects of igneous rocks of the KVPC. According to the technological test results of large-volume samples, significantly high concentrations of platinoids were detected, reaching industrial significance criteria (Pt + Pd + Ru + Rh + Ir = 8–20 ppm). The concentrations of gold and silver are relatively small and in total do not exceed 2–3 g/t with a clear predominance of the latter element [16,26].

4.4. Age Characteristics of the Kresty Volcano–Plutonic complex and Its Correlation in Polar Siberia

The age of the alkaline rocks of the Maymecha-Kotuy Alkaline Province has been considered by many authors who have studied this Province. It is generally believed that the magmatism there is of short duration and occurred during the formation of rift structures on the Siberian craton and adjacent territories [1,7–9,26,34–37]. In many respects, the findings of researchers are quite similar and reflect the already recognized concept of widespread magmatism and associated volcanism, which led to mass extinction at 250 Ma [2,38,39]. An important outstanding gap in the knowledge with respect to Siberian LIP-related magmatism concerns the age of alkaline syenites and granosyenites, which were initially considered final phases of the impact of mantle melts on continental crust rocks. In this case, we show the results of geochronological dating of the main intrusive phases of the KVPC which include the olivinite–wehrlite–clinopyroxenite complex of normal alkalinity, kugdites representing alkaline ultrabasites and melting products of the continental crust material in the form of dykes with syenite composition.

The first geochronological data on KVPC were obtained by the Sm-Nd isochron method for a first-phase ultrabasite series of normal alkalinity, which yielded a result of 251 ± 25 Ma at MSWD = 0.83 (MSWD-mean squared weighted deviation) (Figure 9). In this case, the age determination errors are quite substantial, but appropriate for the method [13]. The age determination assumes narrow variations in the $\varepsilon Nd(T)$ at the level of +1.99–+2.07. Thus, the calculated model age for the ultrabasite series of normal alkalinity of KVPC is in the range of $T_{Nd}(DM) \approx 0.64$–0.79 Ga (Supplementary Materials, Table S2). For example, studies of the $^{187}Os/^{188}Os$ isotope system [40] have shown that the approximate age of ruthenium–iridium–osmium mineralization of the central block of the Guli pluton (Figure 3) is in the range of 545–615 Ma, and its southwestern fragment has an older reference dating (745–760 Ma). The remaining results of Sm-Nd and Rb-Sr isotope studies of the different rock associations of the KVPC did not allow us to yield true isochrons, because only single, whole rock samples were studied. The studying of Sm-Nd and Rb-Sr isotopic systematics was necessary to determine the sources of the substance of the KVPC intrusions in the Maymecha-Kotuy Alkaline Province of, Polar Siberia. These data are discussed in detail in the next section (Section 4.5).

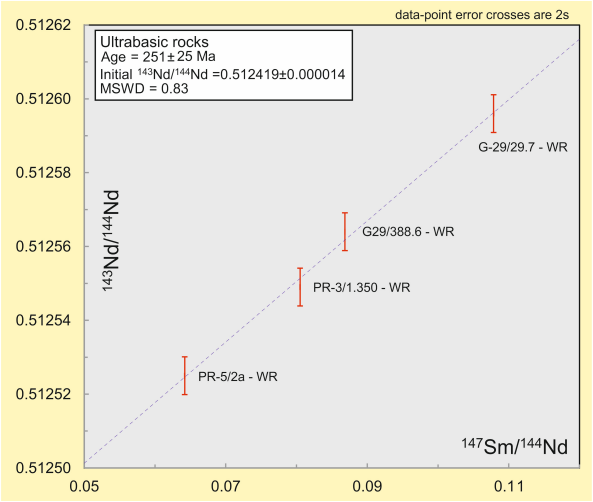

Figure 9. Sm-Nd whole-rock isochron plot for compositions of ultrabasic rocks of normal alkalinity from KVPC.

The determination of the age of crystallization of KVPC magmas was obtained from the results of U-Pb dating of single perovskite grains extracted from Kugdite (Trench No. 3 in Figure 3), which is the second intrusive phase of melilite-containing KVPC rocks (Figure 10).

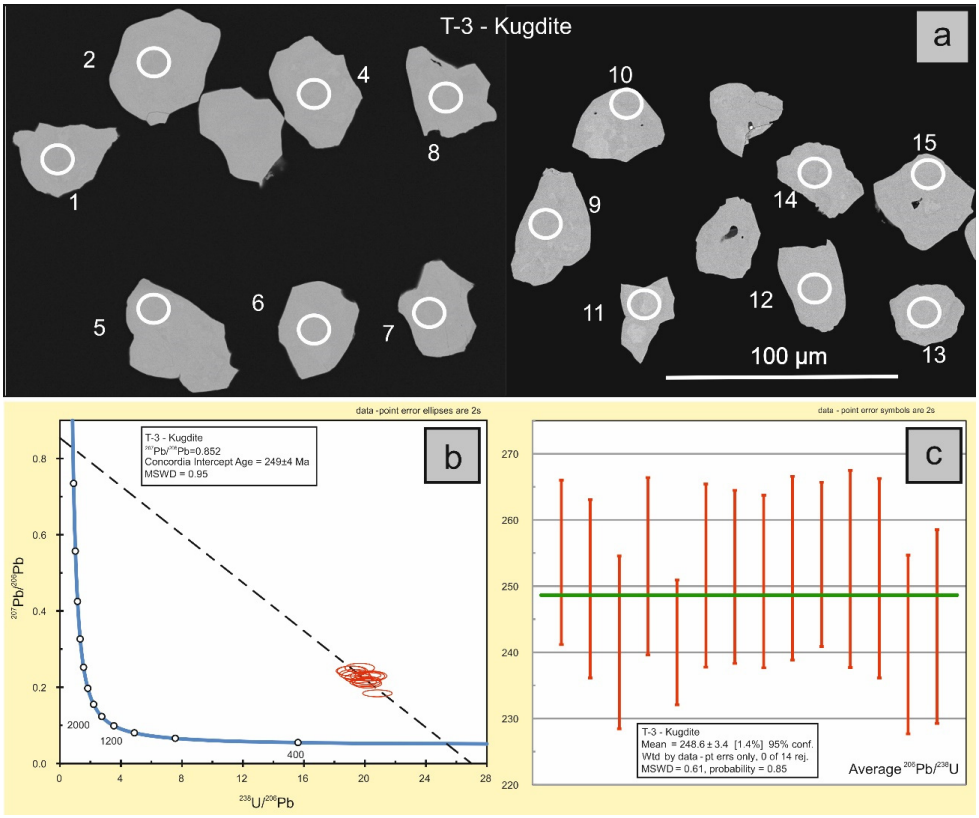

Figure 10. Results of U-Pb dating of perovskite from kugdites (sample T-3) of the KVPC: (**a**)—BSE image of single grains of perovskite with the locations of each isotopic spot analysis circled; (**b**)—$^{207}Pb/^{206}Pb$ concordia intercept age of perovskite = 249 ± 4 Ma; (**c**)—weighted average calculated age relative to $^{206}Pb/^{238}U$ for single grains of perovskite = 248.6 ± 3.4.

Given the absence of zoning and the position of the analyzed points in the central and marginal parts of the grains, these represent adequate geochronological data for this sample (sample T-3). A similar U-Pb perovskite age of kugdites was obtained earlier for the A1103-10 sample during a preliminary study of KVPC rocks. The age of this sample corresponds to a concordia U-Pb age of 248.5 ± 1.3 Ma at MSWD = 0.19 (Figure 11) (Supplementary Materials, Table S3).

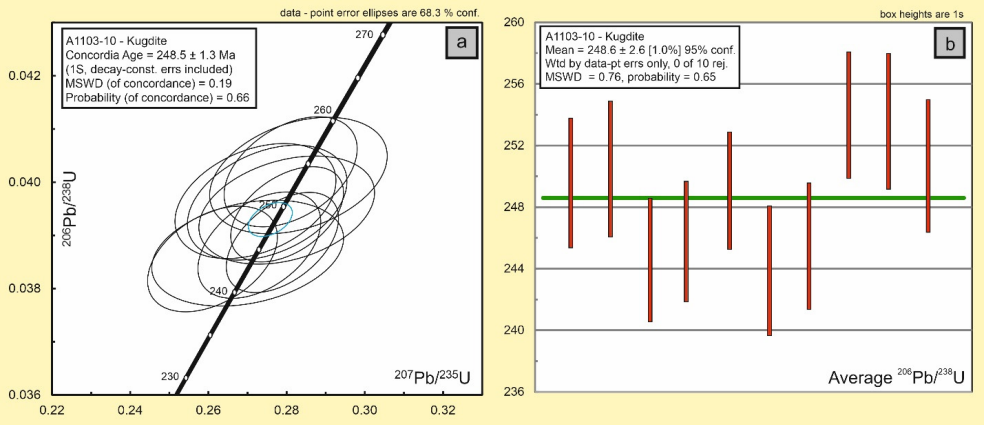

Figure 11. Results of U-Pb age determinations of perovskite from kugdites (sample A-1103-10) from the KVPC: (**a**)—concordant $^{206}Pb/^{238}U$ age of = 248.5 ± 1.3 Ma; (**b**)—weighted average calculated age relative to $^{206}Pb/^{238}U$ for single grains of perovskite = 248.6 ± 2.6.

Dating the most acidic dykes, as represented by syenites and granosyenites of increased alkalinity, is a separate aspect of the geochronological study of the KVPC formation. The dating of syenite dykes permits us to constrain the timing of the final stage of magmatism associated with the formation of the KVPC.

The dating of syenites was carried out on the rocks of two dykes crosscutting ultrabasic rocks of normal alkalinity, i.e., a banded series of olivinite–wehrlite–clinopyroxenite rocks. Dykes were recorded in drill core 29 at depths of 283 and 390 m (Figure 3). They are characterized by typical intrusive contacts. The thickness of the bodies is from 3 to 8 m. Zircon was used as a mineral for geochronological studies. These zircon grains are characterized by pronounced zoning, which emphasizes a likely magmatic origin (Figures 12a and 13a), but it is still enigmatic in these mantle-derived systems and likely requires an elevated pressure (>0.5 GPa) for its stabilization in mantle-derived magmas [41]. Age measurements were carried out in both central and marginal parts of the grains. Isotopic analysis of U, Th and Pb in zircon from syenite dykes from two samples of the KVPC was carried out at nine points for each rock (Figures 12a and 13a).

In order to determine the age of the syenite dykes, representative samples of zircons were selected based on their crystal habits and zonality, as well as a relative lack of structural defects. Since there may be some defects in the internal structure of zircons, like cracks or other deformations, inclusions may be present, thereby distorting the isotopic content of U, Th and Pb. Therefore, the structure, habits and the internal integrity of zircons were analyzed in detail on cathodoluminescent images for the best sampling. According to our analysis of syenite dyke sample G-29-283.3 from the KVPC, we obtained a $^{206}Pb/^{238}U$ age determination of 249 ± 1 Ma at MSWD = 0.26 (Figure 12b). The weighted average $^{206}Pb/^{238}U$ age for single zircon grains based on nine spot measurements was 248.6 ± 1.2 Ma at MSWD = 0.85 (Figure 12c). In the second sample of syenite G-29-390 of KVPC, the concordia $^{206}Pb/^{238}U$ age was 252 ± 1 Ma at MSWD = 0.0037 (Figure 13b). The average weighted age obtained by the isotopic method $^{206}Pb/^{238}U$ for single zircon grains on the basis of nine spot measurements was 252.2 ± 1.8 Ma at MSWD = 1.7 (Figure 13c). Tables with measured contents of Pb, Th and U can be seen in the additional materials of the presented studies (Supplementary Materials, Table S3). It should be added that in

Figures 12a and 13a, smaller zircons have minor defects in the form of fragments and small cracks and therefore they have not been analyzed. At the KVPC, syenite dykes crosscut the bodies of ultrabasic rocks and in these rocks, no zircons were found. We presume that these zircons were not inherited from the host ultramafic rocks, but it is possible that captured zircons from the materials of the underlying crust are present among them, and in that case their age would be older. To further clarify this, additional research is needed. The obtained ages indicate a rather narrow time interval for the main types of rocks of the KVPC, which confirms the theory that the KVPC is intricately related to the 250 Ma Siberian LIP [2,38,39], which heralded the Earth's largest extinction event.

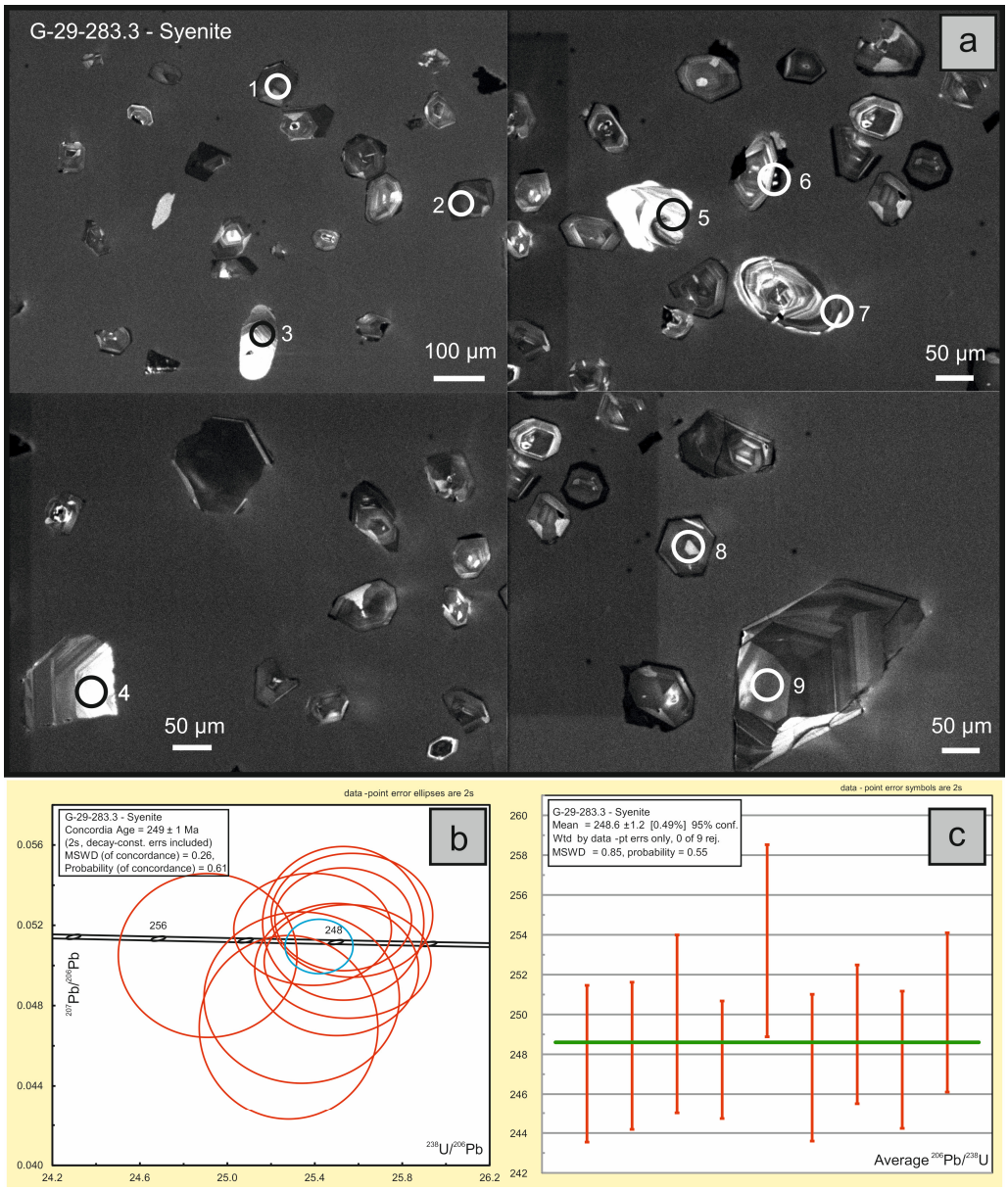

Figure 12. Results of zircon U-Pb geochronological analysis from syenite dykes (sample G-29-283.3) of the KVPC: (**a**)—cathodoluminescent image of single grains of zircon with locations of each isotopic spot (1–9) analysis circled; (**b**)—concordant $^{206}Pb/^{238}U$ isochron with age = 249 ± 1 Ma; (**c**)—weighted average calculated age relative to $^{206}Pb/^{238}U$ for single grains of zircon = 248.6 ± 1.2 Ma.

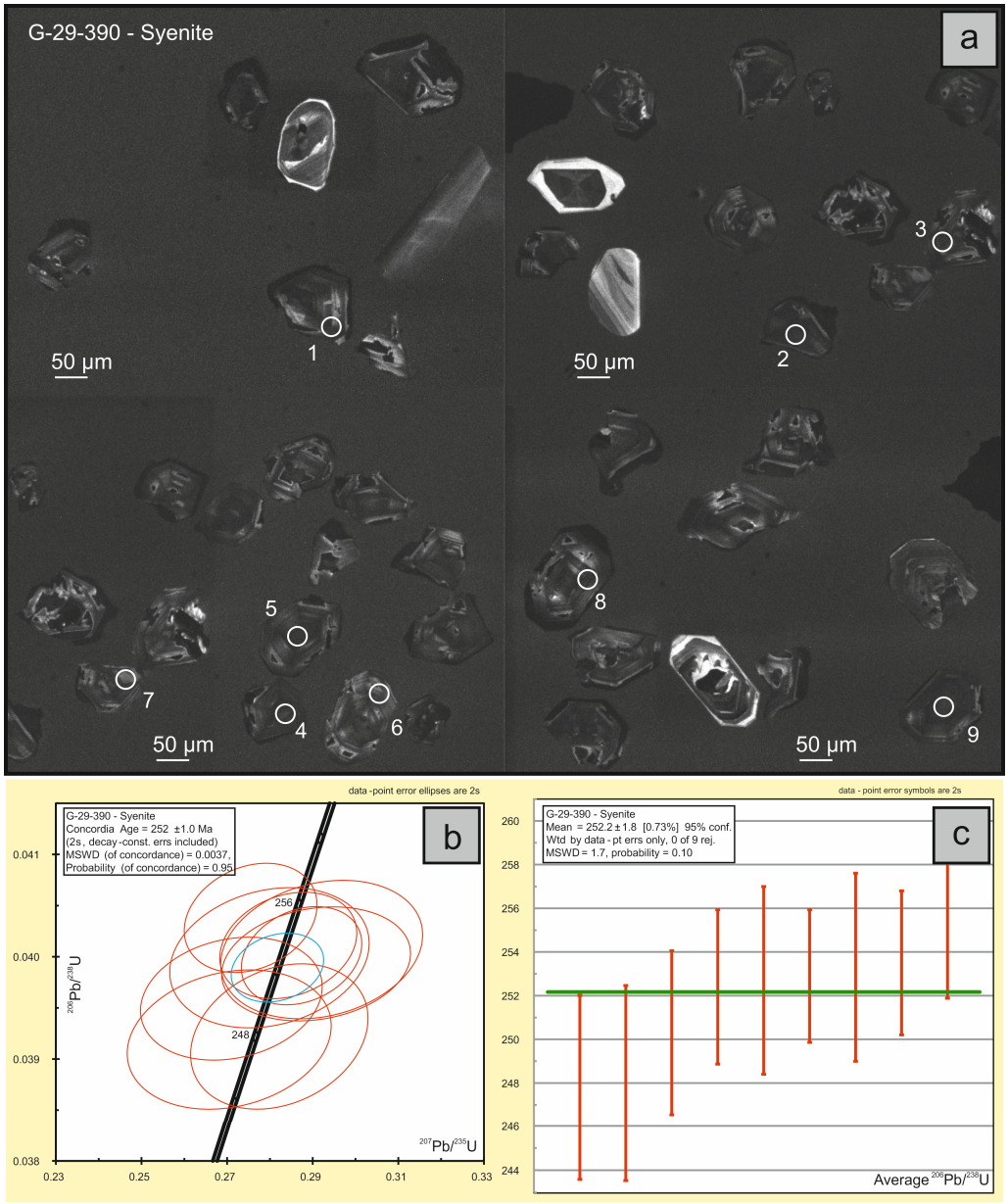

Figure 13. Results of zircon U-Pb geochronological analysis from syenite dykes (sample G-29-390) of the KVPC: (**a**)—cathodoluminescent image of single grains of zircon with locations of each isotopic spot (1–9) analysis circled; (**b**)—concordant $^{206}Pb/^{238}U$ isochron with age = 252 ± 1 Ma; (**c**)—weighted average calculated age relative to $^{206}Pb/^{238}U$ for single grains of zircon = 252.2 ± 1.8 Ma.

In order to correlate the ages of alkaline–ultrabasic magmatism in the Maymecha-Kotuy Alkaline Province in Polar Siberia, we present summary data for the results of geochronological studies by various authors accumulated over several decades (Table 1) [1,13,17,34–36,42]. In general, they fit into a rather narrow time interval and correspond to the Induan stage of the early Triassic, according to [43]. Despite this, there are still small differences between the obtained dates in the Table 1 given. This can be explained by the chosen method of isotope dating and the closure temperature of each isotope system, as well as possible inter-laboratory errors when performing analytical studies.

Table 1. Correlation age of the ultrabasic-basic and alkaline rocks of the Polar Siberia.

Suite/Complex	Rock Type (Mineral/Whole Rock)	Dating Method	Age, Ma	Reference
Maimecha Suite	Meimechite (Biotite)	$^{40}Ar/^{39}Ar$	246 ± 1.2	[42]
Delkanskaya Suite	Meimechite (Zircon)	$^{238}U/^{206}Pb$	251.1 ± 0.3	[1]
Arygdjan Suite	Meimechite (Perovskite)	$^{238}U/^{206}Pb$	251.7 ± 0.4	[1]
Arygdjan Suite (low part)	Melanonephelinite (Whole rock)	$^{40}Ar/^{39}Ar$	253 ± 2.6	[34]
Guli Complex	Carbonatite (Baddeleyite)	$^{238}U/^{206}Pb$	250.2 ± 0.3	[1]
Guli Complex	Bulk (Whole rock)	$^{238}U/^{206}Pb$	250 ± 9.0	[35]
Delkanskaya Suite	Tuff (Whole rock)	$^{238}U/^{206}Pb$	251.9–251.5	[17]
Arygdjan Suite	Lava (Whole rock)	$^{238}U/^{206}Pb$	252.3–252.2	[17]
Guli Complex	Carbonatite (Thorianite)	Th/Pb	250.1 ± 2.9	[36]
Guli Complex	Carbonatite (Baddeleyite)	$^{238}U/^{206}Pb$	250.8 ± 1.2	[36]
Kresty Complex	Olivinite, Wehrlite, Clinopyroxenite (Whole rock)	$^{147}Sm/^{144}Nd$	251 ± 20	[13]
Kresty Complex	Alkaline Syenite (Zircon)	$^{238}U/^{206}Pb$	249 ± 1.0	[This study]
Kresty Complex	Alkaline Syenite (Zircon)	$^{238}U/^{206}Pb$	252 ± 1.0	[This study]
Kresty Complex	Kugdite (Perovskite)	$^{207}Pb/^{206}Pb$	249 ± 4.0	[This study]

4.5. Conditions for the Formation of Intrusions

Studying the structure, petrography, geochronology and geochemistry of the Kresty massif and the host volcanic strata makes it possible to define this geological structure as a kind of volcanic–plutonic association of the KVPC in the Maymecha-Kotuy Alkaline Province. One of the highlights of studying intrusive phases is the contrasting composition of the derivatives of two magma series. The first corresponds to products of normal alkalinity in "olivinite–wehrlite–clinopyroxenite" and the second corresponds to high-calcium magma producing crystallization variants of kugdites, melilitolites and monticellitolites [44]. Various component diagrams (Figure 14) were used to determine probable paleogeodynamic environments and mantle sources [45]. It should be noted that in many parameters, the studied rocks correspond to OIB-type basalts or mantle plume products (Figure 14). We should note some deviations in the criteria for the presented diagrams and especially for geochemical specialization reflecting the influence of subduction or collision processes. In this case, we should talk about the rather complex paleogeodynamic processes that influenced the formation of alkaline–ultrabasic magmatism in the region. Undoubtedly, the primary driver of KVPC magmatism was the involvement of the Siberian Superplume [2,6]; however, it additionally could be influenced by prior accretionary processes at earlier stages of continental crust formation in the region.

At the boundary of the Middle Paleozoic, there was a collision between the Taimyr terrane and the Siberian craton [46]. Subsequent mantle plumes might have interacted with rocks of the continental crust and form an accretion lens.

Radiogenic isotope studies are important to ascertain the mantle sources of magmas. The previously obtained results of isotopic Sm-Nd and Rb-Sr studies on magmatic rocks of the KVPC (Supplementary Materials, Table S2) paint a very interesting picture [13,26]. Ultrabasic rocks of the high-Ca series "kugdite–melilitolite–monticellitolite" in comparison with ultrabasic rocks of normal alkalinity (olivinite–wehrlite–clinopyroxenite) reflect a lower degree of crustal contamination and a more depleted mantle source (Figure 15). At the same time, trachydolerites are characterized by a higher degree of contamination with upper-crust (UC) material, and for alkaline syenites, the ratio of the lower (LC) and upper crust (UC) corresponds to approximately the same level.

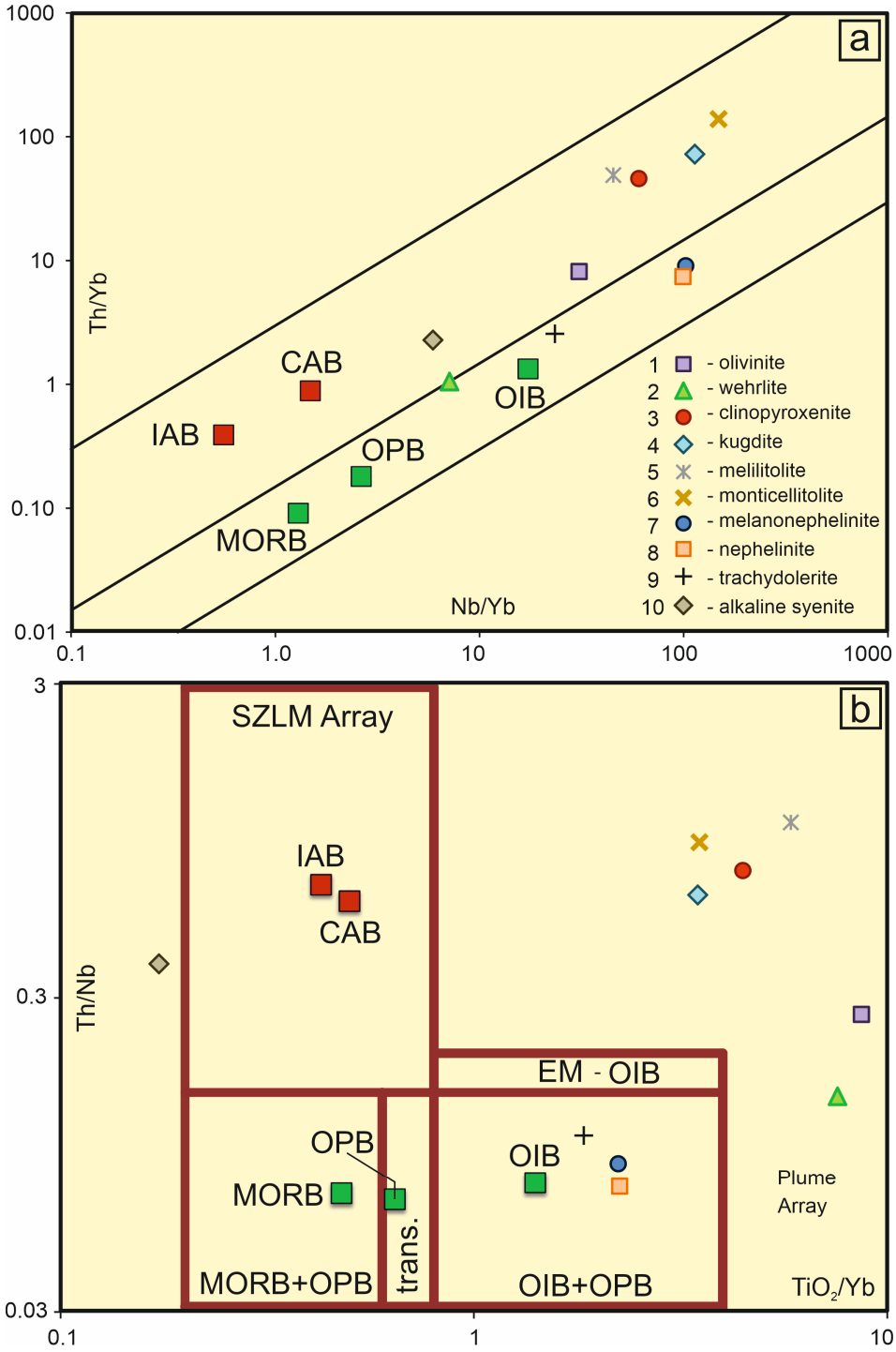

Figure 14. Geochemical characterization of the magmatic rocks of the KVPC using the LIP Printing diagrams of [45]: (**a**)—(Th/Yb vs. Nb/Yb); (**b**)—(Th/Nb vs. TiO_2/Yb). Key: MORB = mid-oceanic ridge basalts; OPB = Oceanic plateau Basalts; OIB = Oceanic island basalts; IAB = island arc basalts; CAB = continental arc basalts; SZLM = subduction-modified lithospheric mantle; EM = enriched mantle [46].

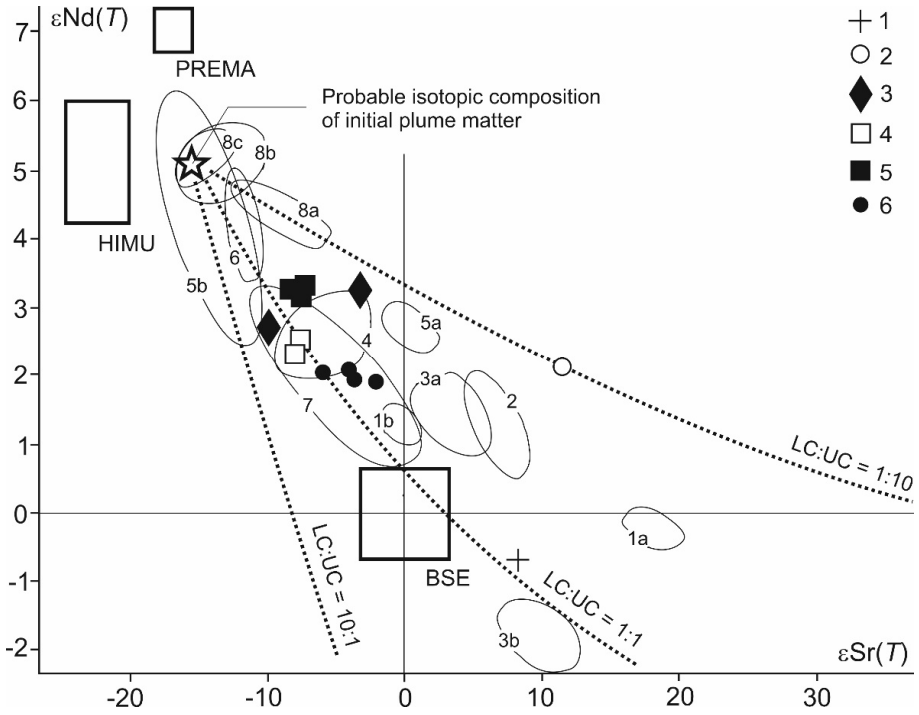

Figure 15. εSr(*T*) vs. εNd(*T*) diagram of the Maymecha-Kotuy Alkaline Province: 1–6: KVPC rocks: 1.—trachyandesite and syenite; 2.—trachydolerite; 3.—melanonephelinite and nephelinite; 4.—melilitolite and hybrid melilite-containing ultrabasite; 5.—monticellitolite; 6.—olivinite–wehrlite–clinopyroxenite complex. The contours show the composition fields of the rocks of volcanic and intrusive rocks of the Maymecha-Kotuy Alkaline Province complexes: 1.—basalts (1a) and limburgite (1b) of the Right Boyar suite; 2. —basalts of the Onkuchan suite (2); 3.—basalts (3a), trachyandesite and trachydacite (3b) of the Tyvankit suite; 4.—nephelinite of Delkan suite (4); 5.—dykes of alkaline picrite (5a) and effusive meimechite (5b) of the Maymecha suite; 6.—carbonatites of the Essei massif (6); 7.—Kugda massif rocks (7); 8.—ultrabasite (8a), melilitolite and foidolite (8b), carbonatite (8c) of the Guli pluton. Isotope parameters of the Maymecha-Kotuy Alkaline Province complexes are shown by former publications [7,8,47–49]. The location of the HIMU, PREMA and BSE mantle reservoirs conforms to their actual parameters [50].

The composition of the main petrological and geochemical varieties of the Maymecha-Kotuy Alkaline Province, reflected in Figure 15, form a compositional field which expands in a fan shape from moderately depleted mantle sources of the HIMU and PREMA types into the area of enriched reservoirs EM-I and EM-II with boundaries along the mixing lines with the substance of the LC and UC in the ratio of LC:UC = 10:1 to LC:UC = 1:10 [13]. At the same time, the isotopic compositions of the derivatives of tholeiitic and alkaline magmas are characterized by noticeable discreteness only at the base of the section of the Mesozoic volcanogenic strata (the Pravobayar, Onkuchan and Tyvankit formations) or in intrusive bodies (the Kugda pluton) and from the supposed focus. As they approach the latter, the compositional fields of igneous rocks move closer and consistently shift to the area of depleted mantle. Similar variations in the isotopic composition with some enrichment with radiogenic ^{87}Sr were also found in the plateau basalts of the Norilsk region [9]. Presumably, this indicates a lower permeability of the mantle substance and its interaction with brines of the sedimentary cover of the platform. Similar results were reflected in studies of alkaline–basite magmatism of the Kuznetsk-Alatau accretionary–collisionary structure and the Altai-Sayan rift system, which are borders of the Siberian craton in the southwest [6,28,51,52].

Volcanic and intrusive rocks of the KVPC occupy an intermediate position between their analogues of the Guli pluton and the Kugda pluton (the location of these objects

is shown in Figure 1) with a relatively weak contrast between alkaline and tholeiitic derivatives. This is quite consistent with the scale of their spatial distance from the probable center of the "finger plume".

Thus, the asthenosphere can act as a source of plume activity, as indicated by the relatively low parameters of $\varepsilon Nd(T)$ at a level of + 5 and $\varepsilon Sr(T) = -15$, a source of the MORB type [48]. Taking into account the extreme depths (200 km) of the origin of the primary alkaline–ultrabasic melts of the Maymecha-Kotuy Alkaline Province [8], the main role of the homogeneous PREMA mantle reservoir is justified in the process of their generation [50]. Deviation from the normal trend in the form of crustal contamination is recorded for later derivatives of alkaline–ultrabasic magmatism (trachydolerites, syenites and granites), during the formation of which interaction with the continental crust or direct melting of the continental crust took place.

The question remains whether crystallization differentiation is probable, where two magmas of different composition could arise—normal alkalinity and high-Ca elevated alkalinity. It was shown that the initial magma during the formation of a specific KVPC association was the initial calcilite melt [53]. Later, using the example of studies of other plutons (the Guli pluton and the Kugda pluton), the authors proposed an intermediate model reflecting either K or K-Na specialization of the primary melt [54], which in our opinion is more acceptable.

5. Conclusions

In this work, we presented a paleogeodynamic model for the alkaline–ultrabasic intrusions of the Maymecha-Kotuy Alkaline Province through the example of the Kresty volcanic–plutonic association. We also considered petrographic, mineralogical and geochemical features of rocks, including isotopic studies and U-Pb geochronological dating. We have shown that the formation of the KVPC association took place in a rather complex setting allowing for the active influence of deep mantle plume and crustal contamination processes in interaction with the crust material from the Siberian craton. Apparently, there was a single mantle source of PREMA-type matter, and the observed diversity of magmatic complexes could be due to the multi-scale plume–lithospheric interaction in the conditions of the rise of melts in the Yenisey–Khatanga rift zone in Polar Siberia. One of the important issues remains the duration of the magmatic process in this region. The obtained ages indicate a rather narrow time duration for the main types of KVPC rocks, which confirms the theory that magmas of the KVPC are related with the Siberian LIP which was active at the Paleozoic–Mesozoic boundary (250 Ma). The given age characteristics of the most recent syenite (249 $\pm$ 1 Ma and 252 $\pm$ 1 Ma) relate only to the formation of ultrabasic series of normal alkalinity, but we should not exclude the possibility of later dykes, crosscutting other phases of igneous rocks of the KVPC and its host volcanic–sedimentary deposits. It is still difficult to invoke fractional crystallization as a mechanism of fractioning melt into two dissimilar melts. For more detailed results, it is necessary to continue studying alkaline magmatism in the Maymecha-Kotuy Alkaline Province, a large block of the Polar Siberia.

Supplementary Materials: The following supporting information can be downloaded at: https://www.mdpi.com/article/10.3390/min14010083/s1. Table S1. chemical and trace element composition in rocks of the Kresty volcano–plutonic complex, Maymecha-Kotuy province, Polar Siberia; Table S2. results of isotopic Sm-Nd and Rb-Sr studies of magmatic rocks of the Kresty volcano–plutonic complex, Maymecha-Kotuy province, Polar Siberia; Table S3. results of isotopic U–Pb studies of zircon and perovskite of the Kresty volcano–plutonic complex, Maymecha-Kotuy province, Polar Siberia.

Author Contributions: Conceptualization, resources and writing—original draft, A.M.S.; writing—review and editing, methodology, software, investigation, visualization and funding, I.F.G. and A.A.M.; validation, formal analysis and resources, T.S.K.; data curation and formal analysis, Y.V.K.; writing—review and editing and methodology, C.G.K.; project administration, V.A.G. All authors have read and agreed to the published version of the manuscript.

Funding: This research was funded by The Tomsk State University Development Programme (Priority-2030, project number IG. 2.0.3.22). The ICP-MS and XRF analysis was funded by the State assignment of the Ministry of Science and Higher Education of the Russian Federation (project number 0721-2020-0041).

Data Availability Statement: Data are contained within the article and Supplementary Materials.

Acknowledgments: The authors are grateful to the staff of the Siberian Federal University (Krasnoyarsk, Russia), the National Research Tomsk State University (Tomsk, Russia), the Institute of Geology and Mineralogy V.S. Sobolev of the Siberian Branch of the Russian Academy of Sciences (Novosibirsk, Russia), Geological Institute—subdivision of the Federal Research Centre, Kola Science Centre of the Russian Academy of Sciences (Apatity, Russia) and the Isotope Research Center of the A.P. Karpinsky Russian Geological Institute (VSEGEI) (Saint Petersburg, Russia) for consulting on the questions for magmatic petrology and performing analytical studies.

Conflicts of Interest: The authors declare no conflict of interest.

References

1. Kamo, S.L.; Czamanske, G.K.; Amelin, Y.; Fedorenko, V.A.; Davis, D.W.; Trofimov, V.R. Rapid eruption of Siberian food-volcanic rocks and evidence for coincidence with the Permian-Triassic boundary and mass extinction at 251 Ma. *Earth Planet. Sci. Lett.* **2003**, *214*, 75–91. [CrossRef]
2. Ernst, R.E. *Large Igneous Provinces*; Cambridge University Press: Cambridge, UK, 2014; pp. 1–667.
3. Surkov, V.S.; Zhero, O.G. *Foundation and Development of the Platform Cover of the West Siberian Plate*; Subsoil: Moscow, Russia, 1981; pp. 1–143. (In Russian)
4. Grinev, O.M. *Rift Systems of SIBERIA: Methodology of Study, Morphotectonics, Minerageny*; Tomsk STT: Tomsk, Russia, 2007; pp. 1–434. (In Russian)
5. Fedoseev, G.S.; Vorontsov, A.A.; Orekhov, A.A. Fossil travertines and quasi-travertine in the Minusa basin (West Siberia): Structure, composition, and comparative analysis. *Russ. Geol. Geophys.* **2017**, *58*, 922–934. [CrossRef]
6. Vrublevskii, V.V.; Gertner, I.F.; Guti'errez-Alonso, G.; Hofmann, M.; Grinev, O.M.; Mustafaev, A.A. Multiple intrusion stages and mantle sources of the Paleozoic Kuznetsk Alatau alkaline province, Southern Siberia: Geochemistry and Permian U–Pb, Sm–Nd ages in the Goryachegorsk ijolite–foyaite intrusion. *Int. Geol. Rev.* **2021**, *63*, 2215–2231. [CrossRef]
7. Arndt, N.; Lehnert, K.; Vasil'ev, Y. Meimechites: Highly magnesian lithosphere-contaminated alkaline magmas from deep subcontinental mantle. *Lithos* **1995**, *34*, 41–59. [CrossRef]
8. Arndt, N.; Chauvel, C.; Czamanske, G.; Fedorenko, V. Two mantle sources, two plumbing systems: Tholeiitic and alkaline magmatism of the Maymecha River basin, Siberian flood volcanic province. *Contrib. Mineral. Petrol.* **1998**, *133*, 297–313. [CrossRef]
9. Hawkesworth, C.J.; Lightfoot, P.C.; Fedorenko, V.A.; Blake, S.; Naldrett, A.J.; Doherty, W.; Gorbachev, N.S. Magma differentiation and mineralisation in the Siberian continental flood basalts. *Lithos* **1995**, *34*, 61–88. [CrossRef]
10. Malitch, K.N.; Belousova, E.A.; Griffin, W.L.; Martin, L.; Badanina, I.Y.; Sluzhenikin, S.F. Oxygen-Hafnium-Neodymium Isotope Constraints on the Origin of the Talnakh Ultramafic-Mafic Intrusion (Norilsk Province, Russia). *Econ. Geol.* **2020**, *115*, 1195–1212. [CrossRef]
11. Marfin, A.E.; Ivanov, A.I.; Kamenetsky, V.S.; Abersteiner, A.; Yakich, T.Y.; Dudkin, T.V. Contact Metamorphic and Metasomatic Processes at the Kharaelakh Intrusion, Oktyabrsk Deposit, Norilsk-Talnakh Ore District: Application of LA-ICP-MS Dating of Perovskite, Apatite, Garnet, and Titanite. *Econ. Geol.* **2020**, *115*, 1213–1226. [CrossRef]
12. Sharma, M.; Basu, A.R.; Nesterenko, G.V. Temporal Sr-, Nd- and Pb-isotopic variations in the Siberian flood basalts: Implications for the plume-source characteristics. *Earth Planet. Sci. Lett.* **1992**, *113*, 365–381. [CrossRef]
13. Gertner, I.F.; Vrublevskii, V.V.; Sazonov, A.M.; Krasnova, T.S.; Kolmakov, Y.V.; Zvyagina, E.A.; Tishin, P.A.; Voitenko, D.N. Isotope composition and magmatic sources of the Kresty volcano-pluton, Polar Siberia. *Dokl. Earth Sci.* **2009**, *427*, 1–7. [CrossRef]
14. Egorov, L.S. *Ijolite-Carbonatite Plutonism*; Nedra: Leningrad, Russia, 1991; pp. 1–260. (In Russian)
15. Chudinova, T.M. *Gravimetric Map of the Krasnoyarsk Territory and Adjacent Areas on a Scale of 1:1,500,000*; Gravimetric Expedition: Krasnoyarsk, Russia, 1993. (In Russian)
16. Sazonov, A.M.; Zvyagina, E.A.; Leontyev, S.I.; Gertner, I.F.; Krasnova, T.S.; Kolmakov, Y.V.; Panina, L.I.; Chernyshov, A.I.; Makeyev, S. *Platinum-Bearing Alkaline-Ultramafic Intrusions of Polar Siberia*; CNTI Publishing House: Tomsk, Russia, 2001; pp. 1–510. (In Russian)
17. Burgess, S.D.; Bowring, S.A. High-precision geochronology confirms voluminous magmatism before, during, and after Earth's most severe extinction. *Sci. Adv.* **2015**, *1*, e1500470. [CrossRef] [PubMed]
18. State Geological map of the Russian Federation. *Scale 1:1,000,000 (Third Generation)*; Norilsk series. Sheet R-47—Heta; Lipenkov, G.V., Mashchak, M.S., Kirichenko, V.T., Naumov, M.V., et al., Eds.; Explanatory note; VSEGEI Cartographic Factory: St. Petersburg, Russia, 2018; 464p. (In Russian)
19. Karmanova, N.G.; Karmanov, N.S. Universal XRF Silicate Analysis of Rocks Using the ARL-9900XP Spectrometer. In *All-Russian Conference on X-ray Spectral Analysis No. 7*; IGM SB RAS: Novosibirsk, Russia, 2011; pp. 1–126. (In Russian)

20. Anoshkina, Y.V.; Asochakova, E.M.; Bukharova, O.V.; Tishin, P.A. Improvement of schemes for chemical sample preparation of carbonaceous rocks with subsequent analysis of high-charge elements by inductively coupled plasma mass spectrometry. *Bull. TSU* **2012**, *359*, 178–181. (In Russian)
21. Williams, J.S. U-Th-Pb geochronology by ion microprobe: Application of microanalytical techniques to understanding mineralizing processes. *Rev. Econ. Geol.* **1998**, *7*, 1–35.
22. Ludwig, K.R. User's Manual for Isoplot/Ex, Version 2.10. In *A Geochronological Toolkit for Microsoft Excel*; Berkley Geochronology Center Special Publication: Berkeley, CA, USA, 1999; Volume 1, pp. 1–46.
23. Black, L.; Kamo, S.; Allen, C.; Davis, D.; Aleinikoff, J.; Valley, J.; Mundil, R.; Campbell, I.; Korsch, R.; Williams, I.; et al. Improved 206Pb/238U microprobe geochronology by the monitoring of a trace-element-related matrix effect; SHRIMP, ID–TIMS, ELA–ICP–MS and oxygen isotope documentation for a series of zircon standards. *Chem. Geol.* **2003**, *205*, 115–140. [CrossRef]
24. Ireland, T.R.; Compston, W.; Williams, I.S.; Wendt, I. U-Th-Pb systematics of individual perovskite grains from the Allende and Murchison carbonaceous chondrites. *Earth Planet. Sci. Lett.* **1990**, *101*, 379–387. [CrossRef]
25. Whitney, D.L.; Evans, B.W. Abbreviations for names of rock-forming minerals. *Am. Mineral* **2009**, *95*, 185–187. [CrossRef]
26. Sazonov, A.M.; Romanovsky, A.E.; Gertner, I.F.; Zvyagina, E.A.; Krasnova, T.S.; Grinev, O.M.; Silyanov, S.A.; Kolmakov, Y.V. Genesis of Precious Metal Mineralization in Intrusions of Ultramafic, Alkaline Rocks and Carbonatites in the North of the Siberian Platform. *Minerals* **2021**, *11*, 354. [CrossRef]
27. Mustafaev, A.A.; Gertner, I.F.; Ernst, R.E.; Serov, P.A.; Kolmakov, Y.V. The Paleozoic-Aged University Foidolite-Gabbro Pluton of the Northeastern Part of the Kuznetsk Alatau Ridge, Siberia: Geochemical Characterization, Geochronology, Petrography and Geophysical Indication of Potential High-Grade Nepheline Ore. *Minerals* **2020**, *10*, 1128. [CrossRef]
28. Mustafaev, A.A.; Ernst, R.E.; Gertner, I.F.; Semiryakov, A.S.; Bilali, H.E.L. Mafic dikes of the Mariinsky Taiga Alkaline Province, Kuznetsk Alatau terrane, southwestern Siberia: Intraplate alkaline magmatism in the Central Asian Orogenic Belt. *Lithos* **2022**, *426–427*, 106799. [CrossRef]
29. Middlemost, E.A.K. Naming materials in the magma/igneous rock system. *Earth-Sci. Rev.* **1994**, *37*, 215–244. [CrossRef]
30. Pearce, J.A. A user's guide to basalt discrimination diagrams. *Geol. Assoc. Can. Short Course Notes* **1996**, *12*, 79–113. [CrossRef]
31. Irvin, T.N.; Baragar, W.R.A. A guide to the chemical classification of the common volcanic rocks. *Can. J. Earth Sci.* **1971**, *8*, 523. [CrossRef]
32. Gűndűz, M.; Asan, K. PetroGram: An excel-based petrology program for modeling of magmatic processes. *Geosci. Front.* **2021**, *12*, 81–92. [CrossRef]
33. Sun, S.; McDonough, W.F. Chemical and Isotopic Systematics of Oceanic Basalts: Implications for mantle Composition and Processes. In *Magmatism in the Ocean Basins*; Saunders, A.D., Norry, M.J., Eds.; Geological Society: London, UK, 1989; Volume 42, pp. 313–345.
34. Basu, A.R.; Poreda, R.J.; Teichmann, F.; Vasiliev, Y.R.; Sobolev, N.V.; Turin, B.D. High-3He plume origin and temporal-spatial evolution of the Siberian flood basalts. *Science* **1995**, *269*, 822–825. [CrossRef] [PubMed]
35. Kogarko, L.N.; Zartman, R.E. New data on the age of the Guli intrusion and implications for the relationships between alkaline magmatism in the Maymecha-Kotuy province and the Siberian superplume: U-Th-Pb isotopic systematics. *Geochem. Int.* **2011**, *49*, 439–448. [CrossRef]
36. Malich, K.N.; Khiller, V.V.; Badanina, I.Y.; Belousova, E.A. Results of dating of thorianite and baddeleyite from carbonatites of the Guli massif, Russia. *Dokl. Earth Sci.* **2015**, *464*, 1029–1032. [CrossRef]
37. Malich, K.N. Complex Platinum-Metal Deposits of Polar Siberia: Composition, Sources of Matter and Conditions of Education. Ph.D. thesis, V.S. Sobolev Institute of Geology and Mineralogy of the Siberian Branch of the Russian Academy of Sciences, Novosibirsk, Russia, 2022; pp. 1–50. (In Russian).
38. Reichow, M.K.; Pringle, M.S.; Al'Mukhamedov, A.I.; Allen, M.B.; Andreichev, V.L.; Buslov, M.M.; Davies, C.E.; Fedoseev, G.S.; Fitton, J.G.; Inger, S.; et al. The timing and extent of the eruption of the Siberian Traps large igneous province: Implications for the end-Permian environmental crisis. *Earth Planet. Sci. Lett.* **2009**, *277*, 9–20. [CrossRef]
39. Wang, T.; Tong, Y.; Huang, H.; Zhang, H.; Guo, L.; Li, Z.; Wang, X.; Eglington, B.; Li, S.; Zhang, J.; et al. Granitic record of the assembly of the Asian continent. *Earth-Sci. Rev.* **2023**, *237*, 104298. [CrossRef]
40. Malitch, K.N.; Badanina, I.Y.; Kostoyanov, A.I. Initial Os-isotopic composition of Os-Ir-Ru alloys from ultramafic massifs of the Polar Siberia. *Dokl. Earth Sci.* **2011**, *440*, 1343–1348. [CrossRef]
41. Borisova, A.Y.; Bindeman, I.N.; Toplis, M.J.; Zagrtdenov, N.R.; Guignard, J.; Safonov, O.G.; Bychkov, A.Y.; Shcheka, S.; Melnik, O.E.; Marchelli, M.; et al. Zircon survival in shallow asthenosphere and deep lithosphere. *American Mineralogist* **2020**, *105*, 1662–1671. [CrossRef]
42. Dalrymple, G.B.; Czamanske, G.K.; Fedorenko, V.A.; Simonov, O.N.; Lanphere, M.A.; Likhachev, A.P. A reconnaissance Ar^{40}/Ar^{39} geochronological study of ore-bearing and related rocks, Siberian Russia. *Geochim. Cosmochim. Acta* **1995**, *59*, 2071–2083. [CrossRef]
43. Gradstein, F.M.; Ogg, J.G.; Schmitz, M.D.; Ogg, G.M. *The Geologic Time Scale 2020*; Elsevier: Amsterdam, The Netherlands, 2020; pp. 1–1390. Available online: https://www.elsevier.com/books/geologic-time-scale-2020/gradstein/978-0-12-824360-2 (accessed on 30 October 2020).
44. Stoppa, F.; Sharygin, V.V. Melilitolite intrusion and pelite digestion by high temperature kamafugitic magma at Colle Fabbri, Spoleto, Italy. *Lithos* **2009**, *112*, 306–320. [CrossRef]

45. Pearce, J.; Ernst, R.E.; Peate, D.W.; Rogers, C. LIP printing: Use of immobile element proxies to characterize Large Igneous Provinces in the geologic record. *Lithos* **2021**, *392–393*, 106068. [CrossRef]
46. Cocks, L.R.M.; Torsvik, T.H. Siberia, the wandering northern terrane, and its changing geography through the Palaeozoic. *Earth-Sci. Rev.* **2007**, *82*, 29–74. [CrossRef]
47. Plank, T.; Langmuir, C.H. The chemical composition of subducting sediment and its consequences for the crust and mantle. *Chem. Geol.* **1998**, *145*, 325–394. [CrossRef]
48. Kogarko, L.N.; Henderson, M.; Foland, K. The Guli Ultrabasic Alkaline Massif in Polar Siberia: Evolution and Isotope Sources. *Dokl. Akad. Nauk* **1999**, *364*, 88–90. (In Russian)
49. Vladykin, N.V.; Morikio, T.; Miyazaki, T. *Problems of Sources of Deep Magmatism and Plumes*; Publishing house of the Institute of Geography SB RAS: Petropavlosk-Kamchatsky–Irkutsk, Russia, 2005; pp. 19–37.
50. Zindler, A.; Hart, S.R. Chemical geodynamics. *Annu. Rev. Earth Planet. Sci.* **1986**, *14*, 493–571. [CrossRef]
51. Vorontsov, A.; Yarmolyuk, V.; Dril, S.; Ernst, R.; Perfilova, O.; Grinev, O.; Komaritsyna, T. Magmatism of the Devonian Altai-Sayan Rift System: Geological and geochemical evidence for diverse plume-lithosphere interactions. *Gondwana Res.* **2021**, *89*, 193–219. [CrossRef]
52. Vorontsov, A.A.; Kovalenko, D.V.; Yarmolyuk, V.V.; Nikiforov, A.V.; Perfilova, O.Y. Geological and isotope-geochemical indicators of plume-lithospheric interactions in the Southwestern frame of the Siberian Craton: Data synthesis for Early Devonian magmatic associations of the Altai-Sayan rift system. *Geol. Geophys.* 2023, in press. (In Russian) [CrossRef]
53. Panina, L.I.; Sazonov, A.M.; Usol'tseva, L.M. Melilite and melilite-containing rocks of the Kresty intrusion (Polar Siberia) and their genesis. *Russ. Geol. Geophys.* **2001**, *42*, 1314–1332. (In Russian)
54. Panina, L.I.; Usoltseva, L.M. Alkaline-ultrabasic mantle-derived magmas, their sources, and crystallization features: Data of melt inclusion studies. *Lithos* **2008**, *103*, 431–444. [CrossRef]